Climatological Perspectives on Fog from the Hibernia Platform

A thesis submitted to School of Graduate Studies in Partial fulfilment of the requirements for the degree

of

Master of Science

Department of Geography, Faculty of Science

by

Elnaz Bodaghkhani

Memorial University of Newfoundland

October 2017

St. John's Newfoundland

Abstract

Frequent advection fog exerts a significant impact on the Grand Banks of Newfoundland and poses a significant hazard to marine and aviation activities. Improved understanding of regional fog processes, climatology, and predictability could offer significant economic and safety benefits. Although this regional fog issue has been recognized for generations, efforts to fully assess the scope of the issue and reduce its impacts have been limited by a lack of long-term, reliable observations of the ocean environment. The advent of offshore oil platforms can help us address this data gap. These platforms provide stationary offshore observations, as they are required to collect visibility data in support of the marine and air traffic that service them. Currently, platform records provide cover 1998 to present. These reports form the primary source of data for our research, and have been used to establish a baseline climatology of fog within the Grand Banks, including descriptions of seasonality and diurnal variability. By treating low visibility events as a point process, the climatology of fog event characteristics including event duration, persistence of fog cover, and coincident weather conditions is further examined. These considerations help identify and classify distinct fog event types and inform preliminary analyses of synoptic climatology. Results are currently being used to guide parallel efforts to develop fog identification and prediction tools for the Grand Banks region.

Acknowledgment

First of all, Thanks to merciful God for all the countless gift you have offered me.

It is a great pleasure to acknowledge thanks to my thesis supervisor Dr. Joel Finnis for his patience and continues support during my Masters study. His guidance helped me in all the time of my research and writing my thesis.

I would also like to thank my husband, family and friends. Without their love and support over the years none of this would have been possible. They have always been there for me and I am thankful for everything they have helped for me achieve.

I acknowledge the AMEC (AMEC Environment and Infrastructure) for providing the data for this project, MEOPAR (Marin Environment Observation and Prediction Response) and Memorial University for funding the research project.

Elnaz Bodaghkhani

Table of Contents

List of Figures

Chapter 1

1.1 Overview/ background:

Frequent and severe advection fog events on the Grand Banks of Newfoundland present a health and safety hazard to marine operations in the region. The severity of the fog problem in Atlantic Canada is evident in maps such as Figure 1, produced by Phillips in 1990, showing the average annual number of days with fog (including mist) over Canada for a 30-year period (1951 – 1980). The highest values (more than 90 days/year) are found along the coast of Nova Scotia and Newfoundland in Atlantic Canada, and regions of the Canadian Arctic Archipelago. Southeastern Newfoundland, located very near the Grand Banks, experiences even higher rates of 150 fog days per year.

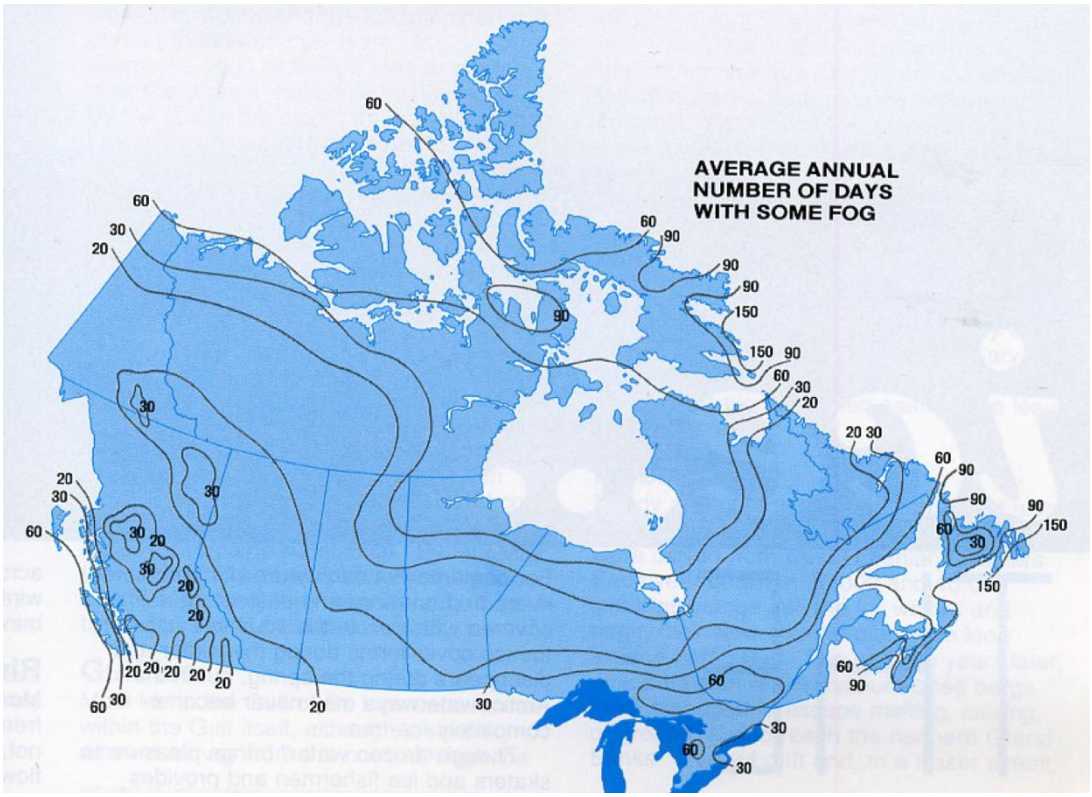

Figure 1 : Annual number of days with some fog (1951- 1980) from Philips (1990)

The advection fog problem on the Grand Banks has been recognized for generations, but an in-depth study of the problem has been limited by data availability. While long-term observations at climate stations have facilitated fog research on land, comparable observations have not been available for the marine environment. Direct fog observations in offshore environments have traditionally been limited to opportunistic observations (rough estimates) of opportunity from vessels that were either outfitted with visibility sensors or had personnel on board that could report weather conditions (Koracin and Dorman, 2001); these are sometimes supplemented by brief field campaigns (e.g. Taylor, 1915; Taylor 1917).

However, this is now changing. The growth of the offshore oil industry provides a new opportunity: offshore oil platforms are required to collect visibility data in support of marine and air traffic moving between Newfoundland and the platforms. These reports will form the primary source of data for this research, as they have been archived for most of the last decade and half.

Observational data from oil platforms have been used to establish and explore the fog climatology in the vicinity of the Grand Banks, giving us an opportunity to quantify the frequency, duration, and severity of fog events and lay the groundwork for prediction efforts. For the first time, a detailed description of the fog problem on the Grand Banks has been produced.

Although the study of fog is complicated, improving the knowledge of fog processes, climatology, and predictability offers significant economic and health/safety advantages. Previous studies on fog suggest that climatological data can help in developing a better understanding of fog formation and forecasting methods (Avotniece et al., 2015; Sugimoto et al., 2013; Kim and Yum, 2010). Studies by Tardif and Rasmussen (2007) and Hansen et al., (2007) suggest that an improved understanding of fog formation requires an exploration of fog climatology; this understanding is itself a necessary first step in improving visibility predictions (Gultepe, Tardif et al., 2007). This research contributes to this effort at the Grand Banks of NL.

The following chapter provides an overview of fog physics and prior research into typology, geography, and climatology.

1.2 Physics of fog and formation processes:

Fog is a collection of suspended water droplets or ice crystals in the atmosphere near the earth surface; it reduces visibility and, in the right conditions, can contribute to icing on manmade structures (aircraft, marine vessels etc). Operationally, fog is normally only reported when it reduces horizontal visibility to less than one kilometer (Van Schalkwyk and Dyson, 2013). However, researchers have often used different definitions based on their study area and goals (Westcott, 2004; Meyer and Lala, 1980). Fog is formed when water vapor condenses near the earth's surface; there are many different processes that can produce this condensation, as well as different processes that can cause its dissipation

(i.e. re-evaporation). Fog is typically classified on the basis of the formation mechanism, and the most common 'types' of fog observed can vary considerably from one region to another. In general, fog is most likely to form if i) there is a strong temperature difference between the ground and the air, ii) the humidity is high and/or there is source of atmospheric moisture nearby, and/or iii) air is experiencing strong cooling. Similarly, fog can be dissipated by i) reducing land/air temperature contrasts, ii) removing moisture from the atmosphere (e.g. through precipitation), or iii) warming air. It may also be formed or dissipated by mixing air with different temperatures and humidity; for example, vertical mixing of dry air aloft with saturated surface air by strong winds is a common fog dissipation/prevention mechanism. A brief overview of fog formation types and dissipation mechanisms follows.

1.2.1 Condensation:

Condensation is the process of converting water vapor to a liquid state. The water vapor amount in the air is extremely variable, as is the air's maximum capacity to hold water. This moisture holding capacity is a function of air temperature, rising as air warms and reducing as it cools. If air is cooled to the point that it cannot retain the moisture it is currently holding, condensation will occur. The air is then warmed through latent heat release, potentially limiting further cooling (and condensation). Therefore, the interaction of temperature and water vapor cannot be ignored in consideration of fog and cloud formation.

1.2.2 Saturation/ Vapor pressure:

Air is a mix of individual gases, with each contributing to the overall gas pressure. The respective individual pressures for each gas are called partial pressure. Water in the form of vapor is a gas, and its partial pressure is called vapor pressure (e).

Air at a given temperature has a maximum proportion of water vapor that it can contain, referred to as the saturation vapor pressure (e_s). If at any point e reaches or exceeds e_s, the air has become 'saturated' and any excess water vapor will be converted to liquid water. In general, the water vapor condenses into liquid faster rather than it could evaporate again. This condensation process leads the humidity toward the equilibrium (saturation) value (Wallace and Hobbs, 2006). This process happens quickly enough that vapor pressure will rarely exceed saturation for long, and relative humidity (e/e_s x 100%) rarely exceeds 101%. That is, air is commonly 'unsaturated' ($e < e_s$), reaches saturation under the right conditions ($e = e_s$), and is rarely and only briefly 'supersaturated' ($e > e_s$).

1.2.3 Claussius-Clapeyron equation:

The relationship between temperature and saturation vapor pressure has been quantified by the Claussius-Clapeyron equation. Separate calculations are necessary for saturation relative to water and ice, but the form most commonly found in introductory texts focuses on saturation relative to liquid water (Wallace and Hobbs, 2006):

$$e_s = e_0 \exp\left[\frac{L}{R_v} \cdot \left(\frac{1}{T_0} - \frac{1}{T}\right)\right]$$

In the Claussius-Clapeyron equation, e_0 = 0.611 kPa, T_0 = 273 K, R_v = 461 J k^{-1} kg^{-1}, and L is specific latent heat;

$$L_{water} = (2500.8 - 2.36\,T + 0.0016\,T^2 - 0.00006\,T^3)\ J/g$$

respectively, these are saturation relative to 0 ^oC water, the freezing point of water, the gas constant for water vapor, and latent heat of vaporization. Other mathematical formulas have been developed; however, all present es as an exponential function of air temperature T. The resulting e_s vs. T curve is shown in Figure 2, and emphasizes that a one-degree temperature change results in much higher vapor capacity change at higher temperatures.

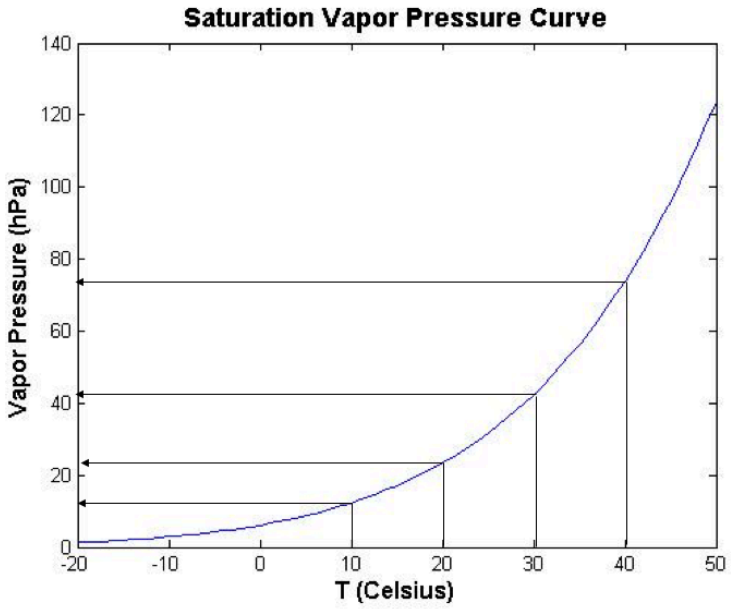

Figure 2: Graph of Clausius-Clapeyron Equation

When the capacity of air to hold water in the form of vapor decreases, in other words when air temperature decreases, condensation will eventual occur. The temperature at which a given air parcel will experience condensation is referred to as the dew point

temperature (*Td*). Under real atmospheric conditions, water vapor needs solid materials and particles for condensation to occur. Therefore, solid particles are necessary elements in the condensation and beginning of fog droplet formation. In practice, there are always sufficient aerosols in the real atmosphere to provide the necessary condensation surface.

In summary, all air contains water vapor of varying quantities. The lower the air temperature, the less maximum capacity for vapor it holds. When air is cooled, relative humidity increases until at a particular temperature (dew point) the air becomes saturated. Any extra water vapor will condense with the temperature dropping below the dew point. As a result of this cooling process occurring close to the ground, fog is formed.

1.3 Types of fog:

A fog classification scheme was introduced by Willett (1928), based on the cooling mechanism that drives saturation. Not all types of fog can occur everywhere. Generally, in addition to classifying fog based on formation processes, the location where the fog has formed is also an important classification factor (Koracin et al., 2001).

For our current purposes, the initial formation mechanisms are used to separate fog types. The main five types are described below.

1.3.1 Radiation fog:

The most common type of fog addressed in scientific literature is radiation fog, which usually forms when an air mass or the land surface cools through radiative processes. In some regions, it is largely a seasonal phenomenon; e.g., at Cape Town International Airport, radiation fog usually happens during winter nights with a clear sky (Van Schalkwyk, 2011). The exact timing of this seasonality can vary considerably from site to site, however. As a general rule, radiation fog forms overnight under clear skies with weak surface winds, when strong radiative cooling of the land surface leads to sensible heat loss from the overlying atmosphere. It often dissipates shortly after sunrise, when radiative surface heating begins, or with the onset of winds, which pull dry air from above into the fog layer (Tardiff and Rasmussen, 2007). Areas dominated by radiation fog will often show a strong diurnal cycle in their fog climatology, with fog forming overnight and disappearing sometime after sunrise.

1.3.2 Advection fog:

This type of fog forms through the horizontal transport of heat (advection), most often when moist and warm air moves across a cold surface (Tardiff and Rasmussen, 2007). For example, advection fog could form when moist tropical air passes over a cold water in a marine environment or an area covered with snow. It is a common occurrence along sea-surface temperature (SST) boundaries between cold and warm water currents, but may form anywhere a surface temperature boundary is present. Winds can push advection fog well beyond these boundaries; e.g. marine advection fog is often pushed towards

nearby coastal communities. Advection fog can be very persistent, and may last for hours, days or even weeks. For advection fog to disperse, one of the factors that causes its formation needs to change; e.g. heating up the cool surface, changing wind direction, or adjusting the amount of moisture in the air (Koracin et al., 2014).

1.3.3 Evaporation fog:

Evaporation fog forms when cold, dry air passes over warmer water; it can be considered a type of advection fog (cold advection), and is sometimes referred to as smoke or steam fog. It is often seen on lakes or near coastlines. In most affected locations evaporation fog is most common in the early morning during fall or winter, when the humidity is high, winds are light, and the temperature difference between air and water is great. Evaporation fog will often dissipate with an increase in wind speed or when the temperature difference between air and water decreases due to sunlight or warm wind. In the winter, evaporation fog often occurs over waters near the coastline or openings in the Arctic sea ice (Souders and Renard, 1984).

1.3.4 Cloud-base lowering fog (CBL):

In general, CBL fog forms when the atmosphere is very stable and air near the surface is cold. So, in most locations CBL fog happens during the night. This type of fog forms when the top of a cloud cools, usually through radiative processes. As the cloud cools, some of the moisture in the cloud condenses into droplets which cause the base of the cloud to extend downward, until it reaches the surface. CBL fog typically dissipates when air temperatures near the surface increase (Kyle et al., 2003).

1.3.5 Precipitation Fog:

Precipitation fog happens when precipitation encounters air that is close to saturation. When the precipitation near the surface evaporates, the air becomes saturated. This type of fog may dissipate when wind speeds increase, or alternatively, when the temperatures increase in the lower layers (Tardiff and Rasmussen, 2007).

Of these types, advection fog is the most common type affecting the Grand Banks. One of the reasons for high fog occurrences in Newfoundland is the suitable neighboring marine environment, with a nearby convergence of warm and cold ocean currents (Koracin et al., 2014).

1.4 Implication & Impacts of Fog

Decreased visibility due to fog is a hazard to all types of traffic. Its impact has significantly increased during the last few decades due to increasing air, marine and road traffic (Croft, 2003 and Valdez, 2000). The cumulative financial and human losses related to fog and low visibility are now comparable to the losses associated with a single extreme weather event such as a tornado (Allan et al., 2001).

While ships and commercial boats can navigate in low visibility by relying on radar and GPS to reduce marine collisions and avoid groundings, technology cannot solve all problems associated with low visibility on moving vessels. Moreover, radar is not available for terrestrial traffic such as cars and fog remains a major safety concern on the roads, capable of causing multivehicle accidents in urban environments (Whiffen et al.,

2003).

Fog has a significant impact on air traffic. During heavy fog events, flights are often delayed or cancelled. Some forms of fog (e.g. advection fog) can develop relatively quickly, preventing aircraft from landing with little notice and requiring costly re-routing. For these reasons, the timely prediction of visibility at airports has a huge potential economic value (Veljovic et al., *2015*). It has been suggested that accurate forecasting for the JFK airport in New York City (NYC) could save up to $500,000 per fog event (Tardiff and Rasmussen, 2007).

Fog also poses a significant hazard to marine activities. Worldwide, 32% of accidents at sea occur during dense fog events (Tremant, 1987). Another recent study suggests that 70% of marine incidents in Atlantic Canada occur during fog (Wu et al., 2009); this is likely an overestimate, but even half this value would be significant.

1.5 Geography of Fog:

Fog is a very local phenomenon, with topography, surface conditions, and meteorological conditions combining to influence the spatial extent, duration, and severity of fog events, as well the fog types that occur. Many locations are dominated by a specific fog type; however, multiple types occur at most study locations. Because the physical processes and required meteorological conditions vary considerably between fog types, it is often necessary to carefully differentiate between types when studying fog physics or forecasting techniques. This does much to explain the frequent reinterpretation and extensions of fog-typing schemes presented in academic literature, as researchers modify

definitions to reflect the needs of specific geographic locations or user needs. For example, Tardif and Rasmussen (2007) refined a classification algorithm of fog and organized it into 5 types (Precipitation, Radiation, Advection, Cloud-base lowering, and Morning evaporation) that reflect the mechanisms of formation in the NYC region. By contrast, only three of types (radiation, advection and cloud-base-lowering fog) were investigated by Van Schalwyk and Dyson (2013) at the Cape Town International Airport. Similarly, fog events in South Korea were classified using Tardif and Rasmussen's (2007) algorithm with an added advection-radiation type (Belorid et al., 2015).

Variations in land surface and coastal characteristics can also affect the dynamic behavior of fog (Koracin et al., 2005). For this reason, Leipper (1994) and Kim and Yum (2010) suggested additional categories distinguishing between sea fog and coastal fog. They consider coastal fog to form over coastal inland areas, while sea fog forms over marine areas and sometimes extends onto land. It has been further suggested that fog at sea should be divided into cold and warm fog types (Saunders, 1964).

Some researchers have employed typing schemes based on the underlying synoptic conditions driving fog, rather than the specific cooling processes involved. For example, on the west coast of Korea (Incheon International Airport), Kim and Yum (2010) organized fog events into four patterns based on the synoptic condition at the time of fog formation: migratory high pressure, low pressure, North Pacific high pressure and Siberian high pressure. This reflects a move away from a consideration of thermodynamic drivers of fog to an emphasis on the realities of operational forecasting, which typically

focuses first on synoptic scale conditions. Unfortunately, these sorts of synoptic classifications are regionally specific, and need dedicated research to apply in new areas.

The formation and duration of fog is not easy to predict, as many factors are involved in generating and dissipating fog on land and sea. To be able to better forecast fog, establishing long-term fog variability is an important step (Tanimoto et al., 2009). This is often a first step in analyses of fog impacts on various stakeholders (e.g. the agricultural sector; Bendix,2002; Uyeda and Yagi, 1982), with such studies providing helpful information on long-term variability of low-level clouds and fog. Sugimoto et. al., (2013) used 80 years of visibility data to investigate monthly fog frequency and study long-term variation in fog frequency on Hokkaido Island, Japan. A long term variation in local meteorological variables such as air temperature, humidity and wind speed is controlling fog generation in the region of study.

As the work cited above demonstrates, research approaches often vary to reflect the geographic situation of specific study areas. Fog research on the Grand Banks is no exception. Research in the area began in earnest with Taylor's detailed study of marine weather in the Grand Banks (Taylor, 1917). While the primary purpose of Taylor's field campaign was to track iceberg movement, he took the opportunity to collect a range of weather observations which were later applied to fog analysis. This included upper air observation using kites, records of observed fog occurrence, and estimates of warm and cold air advection (Taylor, 1917; Koracin et al., 2014). Taylor's early research illustrates the value of new, detailed observations to improve the understanding of physical fog

processes. His work drew from a set of newly available marine weather observations to gain a sense of overall climatology, and eventually led to a physical model of Grand Banks fog formation. According to him, fog forms due to air blowing from warm water into the cold water of the Grand Banks in all observed cases: that is, advection fog.

1.6 Frequency and Variability in Fog:

A variety of statistical analyses have been applied in the study of fog frequency, likelihood, and variability. Often researchers have restricted analysis to data specific to a small geographic location; therefore, results are geographically specific and should not be used to create a generalized picture of fog in all areas. However, comparing the frequency and timing of fog at a variety of locations provides a useful comparison point for the Grand Banks. A brief summary of relevant studies is presented below.

Many quantitative measures have been used to describe the climatology of fog. One simple, common metric is the average annual and/or monthly number of days with observed fog ('fog days') over any location (Phillips, 1990). For example, the mean annual and monthly number of fog days over 14 stations was studied by Avotniece et. al., (2015) in Latvia. The problem with focusing on a mean annual monthly number of days with fog is that if a day has only one hour of low visibility, it is treated the same way as a day with multiple fog observations (see Chapter 2). For this reason, a more detailed climatology, featuring annual and diurnal variations, is often used. Figure 3 shows a description of the frequency of fog as a function of month and time of day for Shearwater,

Nova Scotia (Gultepe, Pagowski & Reid, 2007). Fog climatology can be a useful operational planning tool for stakeholders affected by low visibility (Hansen et al., 2007), particularly in areas impacted by radiation fog (which demonstrates a strong diurnal cycle), or advection fog driven by diurnal variations in surface winds. Given that the operational concern is whether fog is more or less likely to occur, a strong diurnal cycle can help stakeholders identify the best times to operate while avoiding the hazard. It is important to note that fog normally only happens for a fraction of the time during any given fog event, and the criteria for defining a fog event vary between researchers (Gultepe, Pagowski & Reid, 2007).

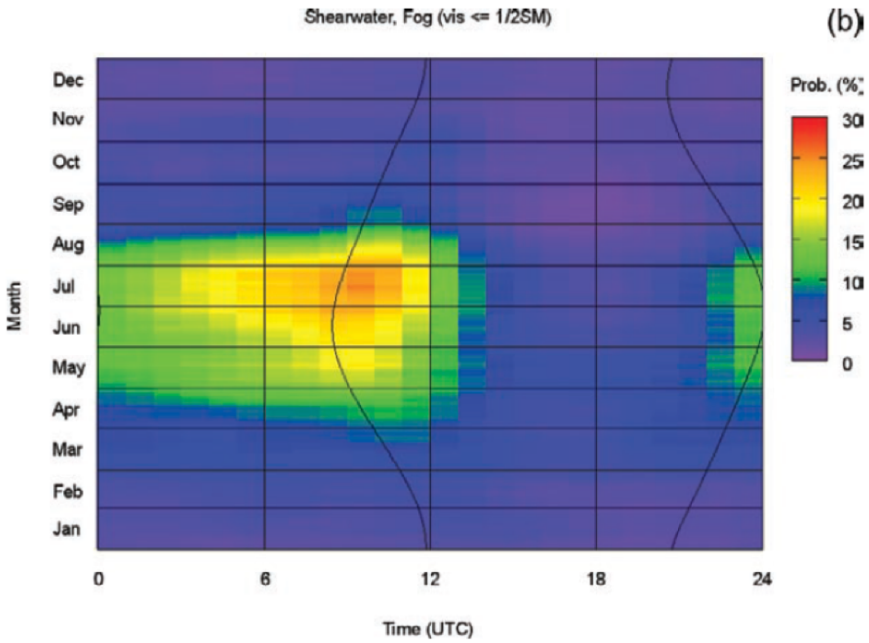

Figure 3: Shearwater, Nova Scotia. The time period covers from 1970 to 2004 with Vis< 1 km. The y axis shows the day and month of the year and x axis shows the time of day. The color bar shows the probability of fog occurrence (Gultepe et al, 2007b)

Some researchers further analyse frequencies of specific fog types. For example, Van

Schalkwyk (2013) investigated the characteristics of three types of fog, further including consideration of minimum visibility and event duration at the Cape Town International Airport. The results showed that radiative processes are the most common cause of fog formation, and further that radiation fog mostly happens in the winter, while CBL fog and advection fog are more likely between March and August. All fog types formed at night and dissipated during the day; however, advection tended to start close to sunrise and showed larger variation in onset times. Similarly, winter fog in the Sacramento area was tested by Suckling and Mitchell (1988) at four sites. They studied the mean number of moderate to dense fog hours, the mean number of fog hours (include light fogs), and the average seasonal minima and maxima. Results showed that the urban sites experienced more fog than other sites; however, urban sites do not necessarily experience greater fog densities (severity). In the NYC region, Tardif and Rasmussen (2007) demonstrated the regional influence of land surface characteristics, with rural areas experiencing more fog events. In NYC, it seems precipitation fog has the longest duration; however, the density precipitation events were less compared to other types of fog. By contrast, radiation fog was marked as the highest density of all types.

Statistical analysis also shows that fog frequency is related to atmospheric circulation and local geographical elements (Cereceda et al., 2002). Climate characteristics of fog formation within 14 major observation stations in Latvia were investigated by Avotniece et al., (2015). The results showed a significant difference in the spatial and temporal distribution of the annual number of days between those observation stations. They investigated associations between fog and other weather variables, such as precipitation

and air temperature at each site. The results showed fog occurring with precipitation, and the trend analysis of fog and air temperature indicated that the decreasing fog frequency in Latvia is associated with an increase in air temperature.

In addition, studies conducted by Veljovic et al., (2015) identify a linear trend in the number of fog events moisture at the Belgrade Airport, along with an increase in the overall number of days with fog during the winter. The temporal distribution of the number of events in the winter time was six times higher than during summer time. Lower visibility at this site mostly happens at night and in the early morning, which suggests radiation fog dominates the area.

Since long term, accurate fog forecasting is not yet available, short-term forecasting of fog events (informed by climatological analysis) remains the focus of most operational forecasting efforts. Hilliker and Fritsche (1999) used climatology for the short-term prediction of ceiling and visibility at the San Francisco International Airport, using surface variables as predictors in the development of a multiple linear regression model. The results showed that the inclusion of upper-air data, which describes the amount of moisture in the boundary layer, may be as important as surface predictors.

1.7 Synoptic Climatology:

Synoptic climatology links atmospheric circulation to different local climates, and studies the relationships between them (Sheridan and Lee, 2011). Furthermore, synoptic

climatology offers approaches to studying and classifying large-scale atmospheric circulation variables into smaller categories of synoptic patterns (Barry and Perry, 2001). A number of previous studies have applied this perspective to the study of fog, tracing synoptic-scale influences back to local scale fog. These efforts recognize that predicting fog formation and dissipation often is not possible using only information on local surface conditions (Lewis et al., 2003). Instead, a broader sense of factors influencing advection, boundary layer depth, or vertical motion are necessary. Again, these synoptic influences are often regionally specific, reflecting local topography and surface conditions, and cannot be easily generalized to other locations. Still, considering the synoptic conditions associated with fog may be critical to better understanding the mechanisms of fog formation in a specific study region.

In a synoptic climatology analyses, sea level pressure (SLP) is the most consistently used climate variable because it represents large-scale atmospheric circulation characteristics. For example, the relationship between large scale atmospheric circulation patterns and precipitation using SLP in Victoria (Australia) was investigated by Pook et al., (2006). However, adding more relevant climate variables in marine fog studies such as skin temperature, which shows the strength and position of ocean currents, could represent the large-scale fog forcing more accurately. In fact, variables that describe surface temperature distributions are often employed in synoptic fog analyses. At sea, relationships between sea surface temperatures (SST) or ocean skin temperatures and dew point temperature (Td) can be among the most useful fog indicators. Typically, these are combined with some analysis of circulation, such as sea level pressure (SLP) fields. Over

the U.S. West coast, strong SST gradients in the presence of northwesterly flow combined with synoptic-scale subsidence associated with an anticyclone are important elements in generating fog (Koracin et al., 2001). Koracin et al., (2005) indicated in their simulation that radiative cooling related to warm, dry air or moist, cool air at the marine layer could be another important mechanism in fog formation. Other studies emphasize the role of temperature differences between the sea surface and overlying boundary layer air, and the influence of strong tidal mixing in coastal fog (Choi et al., 2000). Weather patterns favorable for dissipation are also often examined. For example, Choi et al., (2000) connect the formation and dispersal of advection marine fog in the Yellow Sea to the passage of low pressure systems.

Recent studies have either employed Kohonen's self-organizing map (SOM) to perform a detailed synoptic climatology of atmospheric circulation and fog (Van Schalkwyk et al., 2013), or addressed the possibilities of this technique for regional fog analyses (Tymvios et. al., 2008). The SOM approach in terms of synoptic climatology allows a large number of synoptic patterns to be compared and connected to specific phenomena to to better visualization of synoptic events. In this way each synoptic pattern could be referred to one of the nodes in SOM map, which can be helpful in investigating those phenomena (Cavazos, 2000; Hewitson and Crane, 2002; Reusch et al., 2005). In recent years several studies have been done based on SOM in synoptic climatology to validate the general circulation models (Brown et al., 2010; Finnis et al., 2009; Higgins and Cassano, 2010). Beside application SOM in climate models, some other SOM based studies have focused on precipitation and atmospheric circulation (Cavazos, 2000). In other study the

variability of growing season has been identified in southern Africa by applying SOM on precipitation data (Tadross et al., 2005).

In the context of fog, Van Schalkwyk et al., (2013) used SOMs to examine synoptic circulation patterns related to foggy days at the Cape Town International Airport. They have identified that radiation fog is most frequent fog in the region due to radiative and advective processes. Moreover, the fog at that study area could form due to influence of a low on the southwest coast and high over the South Africa (Van Schalkwyk et al., 2013).

The current study will build on previous synoptic climatological analyses, employing SOMs and canonical correlation analysis to explore synoptic-scale fog influences. These approaches were used to categorize daily synoptic sea-level pressure and skin temperature patterns for the Grand Banks. Further analysis focuses on fog events by using SOMs to identify synoptic situations associated with high fog frequency for the month of April to August (the typical Grand Banks fog season).

1.8 Summary:

Frequent fog events pose significant hazard and safety issues to industries and residents in effected areas. Fog forms and develops due to multiple local microphysical, dynamic, and radiative processes; these are in turn influenced by boundary layer and synoptic-scale meteorological conditions (Gultepe, Tardif et al., 2007a). The ways these various influences work in combination and opposition varies considerably between locations, and consequently understanding fog and improving predictability typically requires

detailed research on specific locations of interest. The current study focuses on improving our understanding of fog in the region of the Grand Banks of Newfoundland; it represents a first step towards the goal of improving operational fog prediction, which may be used for planning purposes and operational decision-making (e.g. planning offshore helicopter flights).

The broad features of Grand Banks fog are reasonably well understood. It occurs year round, but is particularly common in summer, when prevailing winds over an ideally situated front between the warm Gulf Stream and cold Labrador Current promote advection fog. However, a detailed study of the problem has been limited by data availability. Previous studies on fog forecasting suggest that collection and climatological analysis of observational data is a key step starting point in efforts to improve prediction, and can inform understanding of fog formation (Hyvärinen et al., 2007). Our goal is to pursue this work using observational data from the Hibernia platform, giving us an opportunity to quantify the frequency, duration, and severity of fog events in the vicinity of the Grand Banks. For the first time, a detailed description of the Grand Banks fog problem based on long-term, in-situ observation has been produced. We further examine the synoptic climatology of Grand Banks fog, by applying the method of self-organizing maps and canonical correlation analysis to connect Hibernia fog events to broader weather conditions.

A detailed description of methods and data is provided in Chapter 2. This is followed by a detailed description of fog climatology as observed at the Hibernia platform (Chapter 3) and synoptic-scale analyses (Chapter 4).

Chapter 2

Data and Methods

This chapter contains a description of all the data sets used in this research, which include climate station observations and atmospheric reanalysis. This is followed by a description of the methodology that was used to investigate i) fog climatology and ii) the broader synoptic-scale climatology of fog on the Grand Banks of Newfoundland.

2.1 Study Area:

The focus of the current project is the Grand Banks of Newfoundland, a collection of merged subsea banks located south-southeast of Newfoundland. Ocean depths are relatively shallow in the area, typically within the 50-100m depth range. Point source data for the region has been taken from the Hibernia platform, an offshore oil platform located approximately 315 kilometers east-southeast of St. John's, Newfoundland and Labrador (Figure 4), with the coordinates 46°45.026′N 48°46.976′W. Hibernia is required to collect meteorological data in support of marine and air traffic moving between Newfoundland and the platform. These reports will form the primary resource of data, as they have been archived for most of Hibernia's 1.5 decades of operation; this is a considerably longer record than it is available from several neighboring platforms (e.g. West Aquarius), and therefore better suited to the exploratory, data-driven methods employed in the current study.

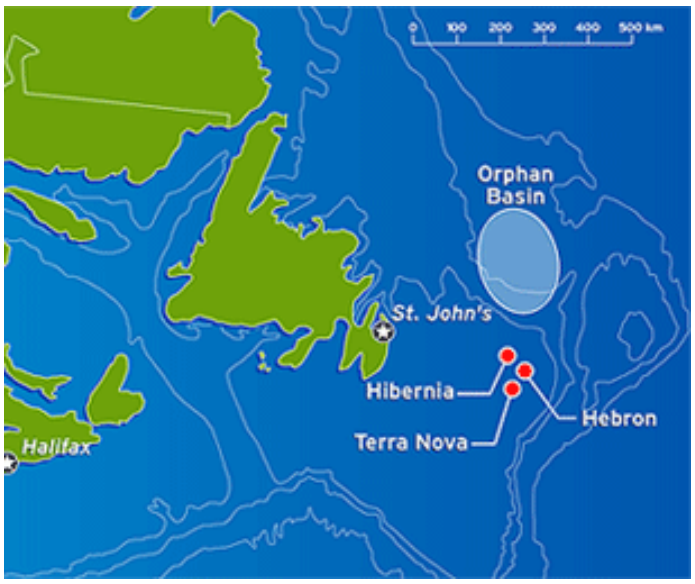

Figure 4 : Hibernia location map (Blag Nosey Parker, 2017).

2.2 Data Sets:

2.2.1 Observational Data:

Hibernia observations come from a weather station and sea surface monitoring equipment located on the platform. Archives have been maintained by AMEC Foster Wheeler, a consulting firm that has provided tailored weather forecasts for Hibernia through most of the platform's operation. While AMEC has used several formats for archiving this data, Marine Meteorological (MANMAR) reports have been used primarily in this study. MANMAR reports are standardized alpha-numeric codes used for reporting weather observations from ocean vessels, ports, and stationary platforms (like Hibernia). They may be prepared by hand, but may also be reported in partial from by automated equipment. MANMAR contains observations on conditions such as weather, cloud cover, temperature, humidity, wind, visibility, and air pressure. These are one of several

meteorological/oceanographic report codes used by the World Meteorological Organization and similar agencies to archive and distribute information efficiently:

> *"Coded messages are used for the international exchange of meteorological information comprising observational data provided by the WWW Global Observing System and processed data provided by the WWW Global Data-processing and Forecasting system. Coded messages are also used for the international exchange of observed and processed data required in specific applications of meteorology to various human activities and for exchanges of information related to meteorology (MANOBS, 2006)".*

Observations for the Grand Banks marine environment over 14 years (1998 to 2014), at 3-hourly intervals (0000, 0300, 0600, 0900, 1200, 1500, 1800 and 2100 UTC) have been used in this study. Specific information extracted from the MANMAR reports include visibility, temperature, dew-point temperature, wind speed, present weather conditions, and weather conditions observed between reports (ie. Conditions 1- and 2- hours prior to the current report). Some of this information is reported directly from measurement instruments (e.g. temperature, winds), but other information is based on the subjective interpretation of a human observer submitting the report. For example, 'weather conditions' can be one of many prescribed categories (e.g. clear, foggy, mixed precipitation etc) noted by the observer at the time of report. While this subjective data can be difficult to interpret, it does contain explicit references to fog and related phenomena (e.g. drizzle) valuable to our analyses.

2.2.1.1 Data Quality:

Due to the mixed objective/subjective nature of MANMAR codes, several corroboration checks and adjustments were performed prior to quantifying Hibernia fog. First, individual observations were checked for consistency across different variables; for example, entries in which fog was reported with low relative humidity (below 95%). Physically inconsistent entries were removed and flagged as 'missing'. In the overall database, 11.51% of entries were removed, and a further 17.26% of entries were missing from the raw data. The years 2003-2005 were also removed from consideration, as these data entries were missing some information required for our analyses. The final quality controlled data set used in the current study covers the fourteen years between 1998-2002 and 2006-2014, with 38.44% missing data.

2.2.2 NCEP/NCAR Reanalysis:

In addition to observational data extracted from MANMAR reports, reanalysis data covering a domain surrounding the study area has been employed. The first NCEP/NCAR Reanalysis, a research-oriented product resulting from the collaboration of the U.S. National Center for Environmental Prediction (NCEP), the U.S. National Center for Atmospheric Research (NCAR), and research partners at many international institutes was selected. This product was selected for its ease of implementation, coincidence with MANMAR observations (4x daily), and because it is as widely used product with a significant history in climate research. The product consists of a continuously updated gridded dataset (Kalnay et al., 1996), providing a wide range of atmospheric variables (air temperature, humidity, pressure, wind velocity, etc.). The data is physically consistent

with available observations and a numerical weather prediction (NWP) model used in the reanalysis process. The data set is effectively a 'best guess' of the atmosphere at a given time, based on prior NWP output and a wide range of available observations. It is available as frequently as 6 hour intervals (from 1948 to present); here, data with latitude/longitude resolution of 2.5° have been used. The data set provides information through the depth of the atmosphere (17 vertical levels), although only surface data has been used here. The reanalysis originally contained two data types; the first type (called an 'analysis' variable) incorporates direct observations, while the second is exclusively a product of a numerical weather model.

Analysis variables used here include the following:

- Air Temperature at 2m above the surface
- Sea Level Pressure
- U/V winds at 10m above the surface
- Skin Temperature
- Specific humidity at 2m

2.3 Methods:

The fog climatology at Hibernia was examined using a combination of simple statistics and a 'declustering' of the data to highlight individual events. Canonical correlation analysis (CCA) and self-organizing maps (SOMs) have been used to study synoptic scale weather patterns in our analyses. The relative likelihood and severity of fog associated with each pattern provide insight into conditions that promote (or prevent) fog in the area, and give guidance for fog forecasting.

In this section, a formal definition of these methods is provided; their application results are described in Chapters 3 and 4.

2.3.1 Data Declustering and Point Process Analysis

Some pre-processing of the data was required prior to analysis. In particular, much of our climatological analysis required the data be 'declustered', moving from individual 3-hourly station data to a sequence of fog events with variable length, separated by fog-free periods. In order to do this, we took inspiration from Point Process statistical models (Brown et al., 2010). These arise from extreme value theory, and provide a means of assessing the expected frequency, duration, and intensity of many extreme weather events. The core ideas are presented below, along with some background on extreme value analysis.

Extreme value theory encompasses a set of statistical tools, useful for analyzing the likelihood, frequency, and/or character of rare, high impact events (Katz et al., 2002; Brown et al., 2010). The most common of these tools are two statistical distributions: i) the Generalized Extreme Value (GEV) distribution, used in the analysis of block maxima (i.e. the largest events recorded in a sequence of time 'blocks', such as annual maxima) and ii) the Generalized Pareto (GP) distribution, used in the analysis of all events exceeding some pre-determined threshold (so called 'peaks-over-threshold', or POT). The two approaches have their respective strengths and limitations. The block

maxima/GEV approach is easy to implement and reduces concerns around autocorrelation, but limits the number of data points used in analysis. The POT/GP approach provides a larger number of events and therefore reduced uncertainty, but may require careful pre-processing of data before use. This may include a semi-objective threshold selection (for 'peaks' identification) and a 'declustering' of data (i.e. grouping consecutive over-threshold observations into longer 'events'). The choice between GEV or GP depends on the data being examined and the questions being asked, but in most cases both will provide some useful information on extremes (Coles et al., 2001; Rauthe et al., 2010).

Another approach to analyzing extremes builds on data declustering and is referred to as a Point Process (PP) model. It builds on the GP/POT to include the analysis of event characteristics, rather than simply the likelihood that an extreme event will occur. Once declustered events are identified, appropriate statistical distributions can be determined for the number of events per year, event duration, peak event intensity, and many other event characteristics a user might be interested in (Coles et al., 2001).

Declustering is a semi-objective process, and requires some careful testing and interpretation (Furrer et al., 2010). Considerations include which thresholds to use to mark the start of an event, what conditions must be met to declare an event over, and how much time is needed to separate two events. For example, a user might need to consider whether a two-hour break in a rainstorm is enough to treat this as two rain events, or if it should be treated as a single (less persistent) event. Setting different declustering

parameters can give very different statistical results, but often additional information can be explored to address some of these differences. In our rain example, a user might widen the length of a 'break' needed to separate events, but add a statistical analysis of event persistence (32 % of the event with no rain).

2.3.2 Canonical Correlation Analysis:

Canonical correlation analysis (CCA) is a tool for exploring statistical relationships between two sets of multivariate data. It has been used in this research to identify possible relationships between synoptic-scale conditions and fog frequency in the vicinity of the Grand Banks, and quantify the relative strength of these relationships. A brief synopsis of CCA follows; readers can refer to Wilks (2001) for more detail.

CCA is a method that has been used widely in climate and atmospheric research (e.g. Xoplaki et al., 2000 and Tippett & Barnston, 2008). As a well-established tool for identifying the statistical relationships between two sets of variables through a joint covariance matrix, CCA has proven useful in forecasting applications (Van den dool, 1994) and diagnosing large-scale atmospheric phenomena (Ward, 1998). In these applications, time series of two or more spatial fields (e.g. sea level pressure and surface temperature) are used to identify maximally correlated spatial patterns; that is, CCA will find the sea level pressure and surface temperature patterns, the strength of which are maximally correlated in time (Rencher, 1992). The procedure can be repeated to extract additional paired patterns, but it needs to be noted that the subsequent pairs must i) be independent of previous patterns (giving a correlation of zero), and ii) the correlation

between paired patterns will decrease with each iteration (Lebart et al., 1984). According to Sirabella et al., (2001), the process can continue until the number of joint pairs equals the dimension of the smaller of the original input fields (Sirabella et al., 2001).

Mathematically, CCA can be described as follows: Consider two physical fields $Y = (y_1, y_2, ..., y_m)'$ and $X = (x_1, x_2, ..., x_n)'$; in the atmospheric sciences, Y is a typically vector of observations collected from n locations, while X is a vector of a second variable, observed at m locations. Given t observations of these fields, CCA looks for vectors a and b that maximize the following: r = correlation ($a'X, b'Y$). Formally, $U = a'X$ and $V = b'Y$, which are referred to as a pair of canonical variables (Bretherton et al., 1992), where a and b have the same dimensions as X and Y, respectively, and can be considered joint patterns of variability in the two original fields. Computationally, a and b can be found through a singular vector decomposition of the correlation matrix between X *and* Y. According to Repelli and Nobre, (2004) CCA is the most powerful method to compare fields in geophysical data. CCA can be a suitable statistical test in diagnosing aspects of the coupled variability of fields.

In this study, CCA was used to identify variables with a strong synoptic-scale association with estimated fog probability, based on MANMAR data as predictors. That is, X was set to the likelihood of fog at Hibernia, and Y was set to a field suspected to influence fog likelihood (Figure 5). Fog probability was used instead of a binary absence/presence, as a continuous variable is better suited to CCA than categorical data. This value was estimated using cross-validated logistic regression; each year was predicted using a logistic regression fit using all other years of data. Trained against Hibernia fog

presence/absence data with Hibernia's air temperature, dew point temperature, and wind speed as predictors, the regressions demonstrated statistically significant ability in estimating fog likelihood (see section 4.1.1 for details). For the purposes of this study, they represent a sufficiently accurate and continuous indicator of fog.

CCA was applied to a number of geophysical fields covering the Grand Banks and surrounding areas, including air temperature, skin temperature of the ocean, sea level pressure, specific humidity, and wind fields ([zonal winds, meridional winds], or [$\boldsymbol{u}$, $\boldsymbol{v}$]). Greater correlation between resulting canonical variables implies a stronger link between fog likelihood (X) and one of these fields (Y); a stronger link implies the field has greater predictive power and may provide insight into physical drivers responsible for advection fog events. It should be noted that CCA is best suited to identifying linear relationships; another method (self-organizing maps) used in this study is suited to identifying nonlinear relationships, should these exist. Results are presented in Table 1 in Chapter.4. A diagram illustrating the relationships between variables is shown in Figure 5.

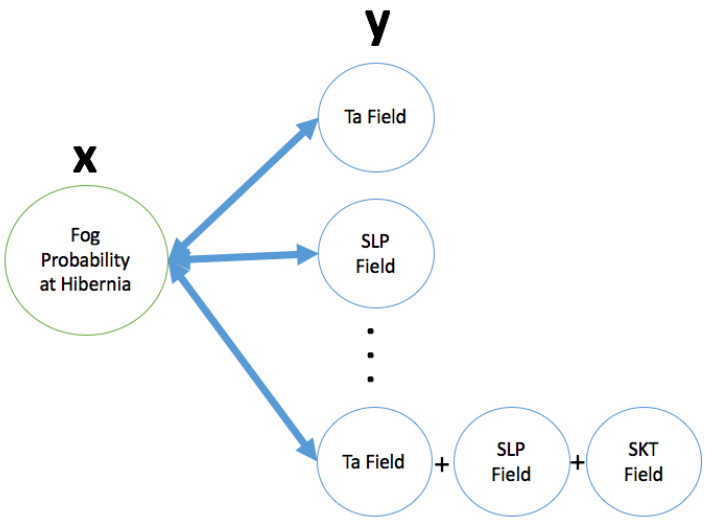

Figure 5 : CCA analysis. A diagram illustrating the relationships between variables. Using logistic regression, Probability of fog at Hibernia = f(Ta, Td, u, v, date, time), where Ta = Air temperature, SLP = Sea level pressure and SKT = skin temperature.

2.3.3 Self-Organizing Maps (SOMs):

The Self-Organizing Map is essentially an unsupervised artificial neural network (ANN) analogue to traditional cluster analysis, based on an algorithm originally introduced by Kohonen (1982). In the SOM process, the whole data set is used to train a simplified version of the original data (a 'map'), consisting of a predetermined number of archetypal data points ('nodes') arranged in a two dimensional lattice. During training, neighboring nodes are adjusted together, encouraging the lattice to adopt an easy-to-interpret order. The SOM algorithm is an unsupervised ANN, in that it doesn't require a target value during training. Because no desired outcome is given, no comparisons are made to predetermine an ideal response. This can be contrasted to supervised ANNs, which attempt to optimize results relative to a predetermined target value; e.g. ANN-based

regression, which will attempt to optimize the estimate of a target (e.g. fog probability) relative to input predictors (e.g. air temperature and dew point). SOMs serve to reduce the dimensionality of data and ease of interpretation, and are often used to explore and interpret large data sets in geophysical sciences (Kohonen, 2001; Alhoniemi, 1997, 1998; Obu-Cann, 2001; Astel et al., 2007).

One of the most attractive aspects of the SOM algorithm is its ability to convert a complex data set into a two-dimensional structure, while preserving the topology of the original data (Back et al., 1998). The SOM process converts high dimensional data to a lower dimensional set, while emphasizing nonlinear statistical relationships and key clusters (Kangas, 1995; Kohonen et al., 1996; Zhang, 2009). In other words, key statistical information is retained and presented in an approachable manner.

2.3.3.1 The SOM Algorithm

A SOM consists of two interconnected layers: a multi-dimensional input layer and an output layer which results from a competitive learning process. The output layer represents a grid of M nodes in a two-dimensional space. The nodes have been defined as i = 1, 2, …, M. These nodes are vectors, with the same length as the input training data. Assume this length is n; then each node i can be represented by an n-dimensional weight vector Mi= [mi_1 …., min]. The weight vectors of the SOM form a codebook: over the course of training, the M nodes can be re-ordered such that neighbouring nodes become

similar, while separated nodes are likely to become increasingly dissimilar (Rustum, 2009).

This idea of neighbouring nodes results from the fact that the output nodes are connected to each other in a two dimensional lattice (topology), the shape of which is selected by the user. This lattice can be either rectangular or hexagonal, depending on the nature of the data and the user's needs. Figure 6 gives some sample lattices, with nodes represented by red circles and connections between neighbours represented by black lines. For the simpler rectangular topology, individual nodes are connected to up to four neighbours, while the more complex hexagonal map connects up to six neighbors. It should be noted that nodes at the edge of the map are exceptional, since they have fewer immediate neighbors (Back et al., 1998; Vesanto et al., 2000).

The number of nodes (M) and the topology (dimensions) of the lattice are subjective, and must be set by a user before training; however, some general guidelines for these choices have been proposed (Alhoniemi, 1997; 1998). One often used rule of thumb suggests that M should be proportional to the number of entries in the training data set (N) (Vesanto et al., 2000; Garcia and Conzalis, 2004):

$$M = 5\sqrt{N}$$

Once M is determined, the relative number of rows to columns in the final SOM output map can be calculated as follows:

$$\frac{l1}{l2} = \sqrt{\frac{e1}{e2}}$$

Where l_1 is the number of rows and l_2 is the number of columns in the final map, e_1 is the biggest eigenvalue of the training data set, whereas the second biggest eigenvalue was identified as e_2. In the above formulas, the logical mathematics and formal theories of determining a SOM's map size have been explained. The map size and quality of the map after training could be also calculated based on quantization error value, which is defined later in chapter 4. Another approach to evaluating the trained map is the Sammon map (Sammon, 1969). This provides a visual representation of the map's 'order'. In this study, the quantization error value has been used in combination with Sammon maps to select map size. The approach is explained in detail in Chapter 4.

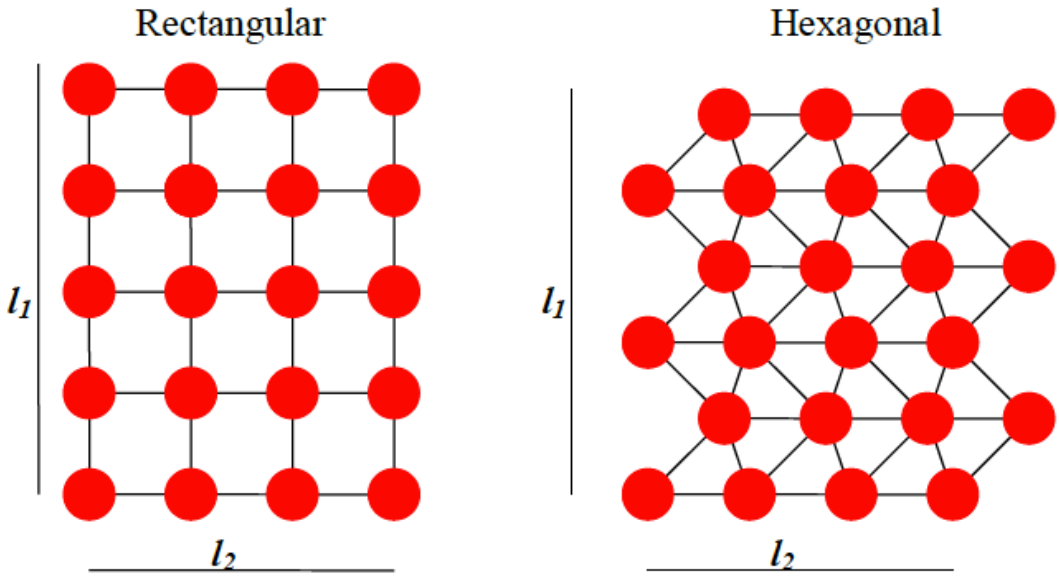

Figure 6: Examples of map topologies in the SOM

2.3.3.2 Training of SOM

In order to train the SOM map, the initial values of the elements of the weight vectors in the grids are randomly assigned. Then the weight vectors are updated through either a sequential (one observation at a time) or batch (multiple observations at a time) training algorithm. Regardless of the approach, both follow the same basic procedure (Rustum, 2009).

In the training process every variable has to be of equal importance. Therefore, it is important to give the same value to each entry point in our original data set and standardize the main data set (input data). In order to do this, the mean has been deducted from each variable in the multi-dimensional data and then divided the result by the standard deviation (following Alhoniemi, 1998).

In each training step, instances from the training data are compared to all of the SOM nodes. The Euclidian distance between the input training vector and node weights is calculated, and the node with the minimum distance (best match) is identified as the 'winner'. Mathematically, the Euclidean distance comparison can be expressed as:

$$Di = \sqrt{\sum_{j=1}^{n}(xj - mij)^2} \quad i= 1,2,\ldots M$$

In above equation, Di is the Euclidian distance between the input vector and the weight (or code) vector i, each with j elements; xj is the current input vector and mij is the weight vector i, and M is the number of neurons in the final SOM (or the size of the map). After determining the best matching unit, nodes within a training 'neighborhood' are identified. These are nodes connected to the winning node by >= r connections in our SOM lattice, where r is the current neighborhood size. For example, if r = 1 in a rectangular SOM, the four nodes surrounding the winner would be included in the neighborhood. The winning and neighborhood nodes are 'activated', and adjusted to better match the input training vector xj:

$$W(t+1) = W(t) + L(t)c(t)[V(t) - W(t)]$$

In this equation, t stands for time, L is a learning rate, V is the input vector, W is the neighborhood function centered in the winning unit at time t (weight), the c(t) defines the region of the influence in that input sample.

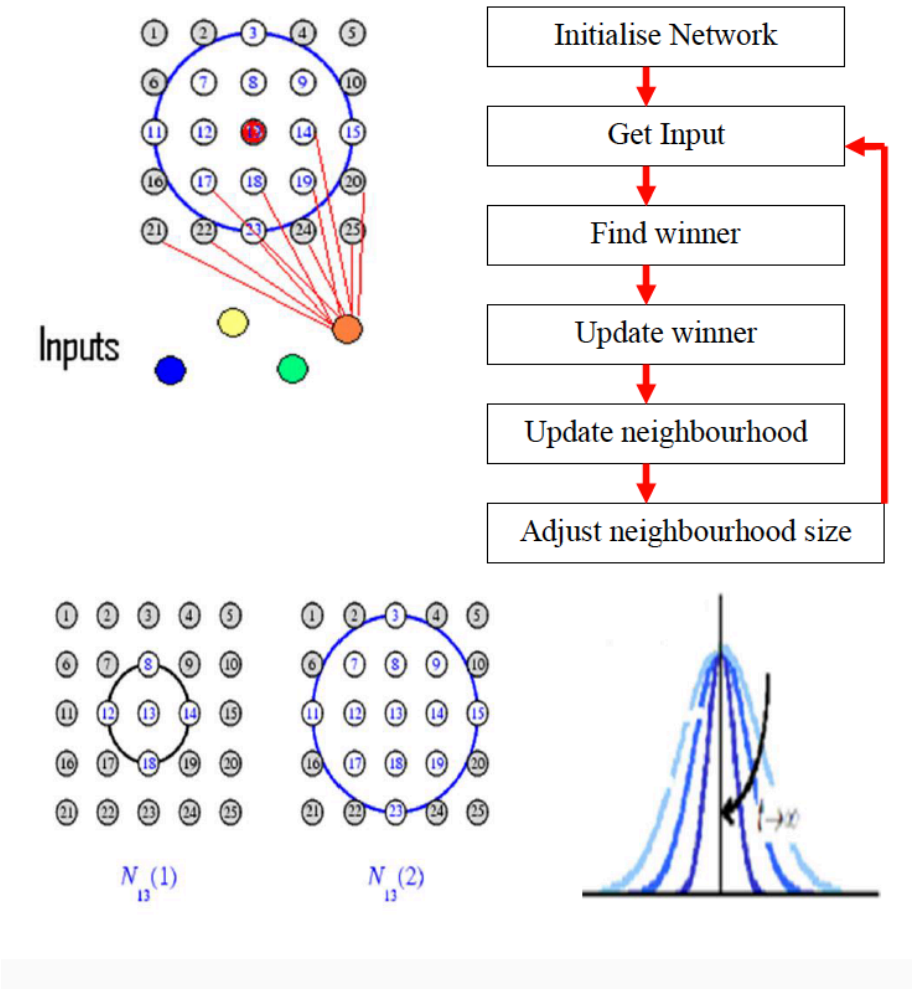

Figure 7 Tthe training procedures of the SOM. Node 13 is the winning node (or Best Matching Unit; BMU); it can be seen how the neighborhood of the BMU (node 13) moves toward the BMU with each iteration. Here, N (2) is a bigger neighbourhood (r = 2), while N(1) is smaller (r = 1). (After Rustum, 2009)

The process of random selection from the data, the competition for the winning node, and updating the winner and its neighborhood is repeated many times; typical trainings will include hundreds of thousands of iterations. As training proceeds, the neighbourhood size and learning rate decrease, gradually approaching one and zero respectively. As a result,

early stages of training will produce large adjustments in the overall SOM, while later iterations result in smaller refinements. By the end of training, nodes in the map will have adopted key characteristics of the input data, and be strongly identified with the input data distribution. This ability of the nodes to adapt as group is labelled as "Self-Organization", since no external force or extension is used to cluster and organize the individual nodes (Penn, 2005).

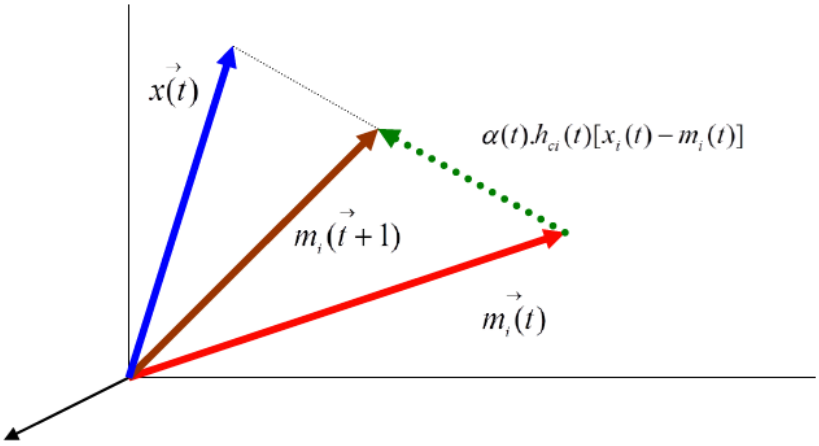

Figure 8: Prototype vector mi (t) of the neuron is updated close to data vector x(t) to be mi(t+1) (After Rustum (2009)).

In this study, SOM analysis was used to explore synoptic scale weather patterns that promote fog and contribute to fog likelihood on the Grand Banks. Further details on our application of the algorithm are provided in Chapter 4.

All statistical and climatological analysis was performed with R version 3.1.1, with the exception of SOM training which was been with SOM-PAK (http://www.cis.hut.fi/research/som-research/).

Chapter 3

3.1 Fog Climatology

Climatological analyses provide a means of quantifying and communicating the scope of Grand Banks fog, both as a weather phenomenon and a hazard for marine workers. By matching scientific questions or stakeholder needs to suitable analysis tools, a foundation for informed operational decision-making and guidance for further research can be built. The following chapter begins this work through several detailed analyses of the Hibernia platform meteorological record. Beginning with the construction of an annual cycle of fog likelihood, the chapter proceeds to establish a Grand Banks 'fog season', explore trends and interannual variability, and examine the climatology of fog events. This represents an important first step towards understanding fog in this unique region, and applies both established and novel approaches to analyzing visibility. All work is based on three hourly MANMAR codes, collected from 1998 through 2014.

3.1.1 Identifying Fog in the Observational Record

Before exploring climatology, first it is necessary to identify fog instances in the Hibernia weather record. This not as simple as it may first sound. Although MANMAR reports include a code describing current weather, it can be difficult to determine what the weather reporter meant when they indicated the presence of fog. Similarly, fog may be superseded by another weather condition (e.g. rain, flurries etc) also present at the time of the report. Fortunately, related variables (e.g. visibility, dew point, and air temperature)

and neighboring entries in a time series can guide interpretation. By testing and selecting appropriate decision rules on the basis of all these factors, the process of identifying fog events can be automated and efficiently applied to long data sets.

After a good deal of testing, the following criteria for identifying a fog event were applied to the data set:

a) Visibility below 4km.

b) Relative humidity above 90%.

c) Fog was reported as a weather condition within a three-hour interval.

The first requirement ensures that any fog is sufficiently severe to require attention. While 4km visibility is not an operational concern, a higher (less severe) threshold has been chosen that would be more useful when exploring physical mechanisms driving fog formation. While other atmospheric characteristics (local warming/cooling, aerosol content, cloud droplet size distribution, and more) can influence the severity of an event, the underlying cause of the fog remains consistent. For this reason, including more fog instances is potentially beneficial to understanding fog phenomenology. The second criterion helps limit our consideration to low visibility during favorable conditions for fog formation. In theory, fog indicates 100% humidity; however, in practice observed humidity might be somewhat lower or higher than this when fog is reported. In some cases, we noticed that fog was reported when humidity was considerably less than 80%. This may occur when fog is visible from the platform, but not present near the climate station. The final criterion provides further evidence that fog is a factor, even if rain, drizzle, or even snow are also factors over the course of an event. The relative

contributions of these factors can vary quickly, with fog present continually but of shifting importance.

Applying these criteria proved successful in removing key problems, including reports of fog during low relative humidity and/or high visibility. A total of 840 entries were found where this was the case, and may have resulted from i) visible fog below or above the platform level, ii) instrument error (e.g. malfunctioning moisture sensors), or iii) reporter error.

3.1.2 Annual & Diurnal Cycles

An estimate of fog likelihood as a function of time of year (annual cycle) and time of day (diurnal cycle) can be made by calculating the fraction of observations (for a given day-of-year and time of day) showing fog. Given the relatively short length of our record, this estimate will be relatively rough and is likely to be sensitive to outliers (e.g. a few very foggy years). Figure 9 shows this rough climatology as gray dots (one per 3 hourly step), using the fog definition outlined in 3.1.1. This was subsequently smoothed using a Fourier filter; the rough results were mapped to the frequency domain using a fast Fourier transform (FFT), and only significantly large frequencies (with sufficient 'power') were kept. In this case, these frequencies included the annual (one-year cycle), the half year (2 per year), the third year (3 per year) cycles and daily fluctuation. Although the impact of daily fluctuation remains small compare to annual, semi- annual and third annual, it was kept to ensure we resolve influences related to solar burn-off of fog.

All other frequencies were removed (set to an amplitude of zero), and the results were

returned to the time domain with a reverse FFT. Results are shown as the black line in Figure 9. A similarly smoothed estimate of error is given by the red lines, based on the standard error over a 5-day moving window of fog frequency; effectively, this gives an estimate of variability over the five-day moving window in our record. Figure 10 shows the same smoothed climatology in another form, to further emphasize the relative size of the annual (vertical axis) and diurnal (horizontal axis) cycles. Results emphasize that choosing any time of day and looking through all dates gives a large shift, while choosing any date and moving through all times of day gives little variation.

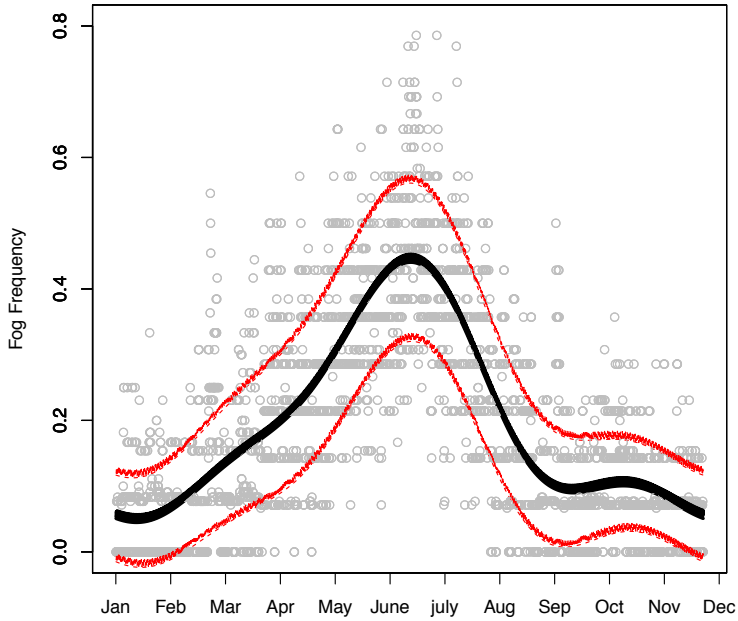

Figure 9 : : Annual Fog climatology, with fog frequency given as a fraction of observations with expected fog (Nfog/Nobservations). Results are shown for 3-hourly intervals, over the course of the year. Raw estimates (unsmoothed) are given as grey dots, and FFT filtered estimate is given as a solid black line. Red lines show one standard error about the FFT mean.

Results show a very strong annual cycle and weak diurnal cycle (Figure 10), with the

annual likelihood passing from less than 10% (< 0.1) to more than 40% (>0.4). Diurnal variations about the annual cycle are relatively small, amounting to a few percentage points of difference. The annual peak falls in June, preceded by a gradual increase from a mid-January minimum. This increase sees a slight plateau in March (~0.2), perhaps related to shifting seasonal influences on fog formation. The reduction in fog likelihood after the peak is more abrupt, reaching a local minimum in September before rising to a small secondary peak in October. The diurnal cycle becomes a little more pronounced in fall, which could point to shifting fog types, and perhaps an increase in the likelihood of radiation or cloud-base lowering fog, which are strongly connected to solar forcing. However, overall the strong annual and weak diurnal cycles suggest Hibernia is dominated by advection fog events.

3.1.3 Fog Season & Interannual Variability

Using this annual cycle, a semi-objective definition of a 'fog season' for the region has been proposed, which can be applied to an individual year's data (Figure 11). Based on the small plateau in the annual cycle graph (early April; beginning of the steep rise to peak season) we chose a threshold marking the beginning of the fog season: an observed fog frequency of 25% over the subsequent 21 days. This corresponds with April 8 in the longterm climatology. The definition is applied by calculating the observed fog frequency for each date/time over the subsequent 21 days; the first day to hit 25% is marked as the beginning of the season. Similarly, the fog season is considered to end on the last date to drop below this threshold. This allowed us to focus on the period after the mid-spring plateau (likely associated with changing fog drivers or surrounding environmental

conditions), and before the mid-Fall secondary peak (October). Figure 11 adds this threshold to Figure 9, highlighting the mean 'season' that runs from April 8 through August 21, giving an average length of 136 days.

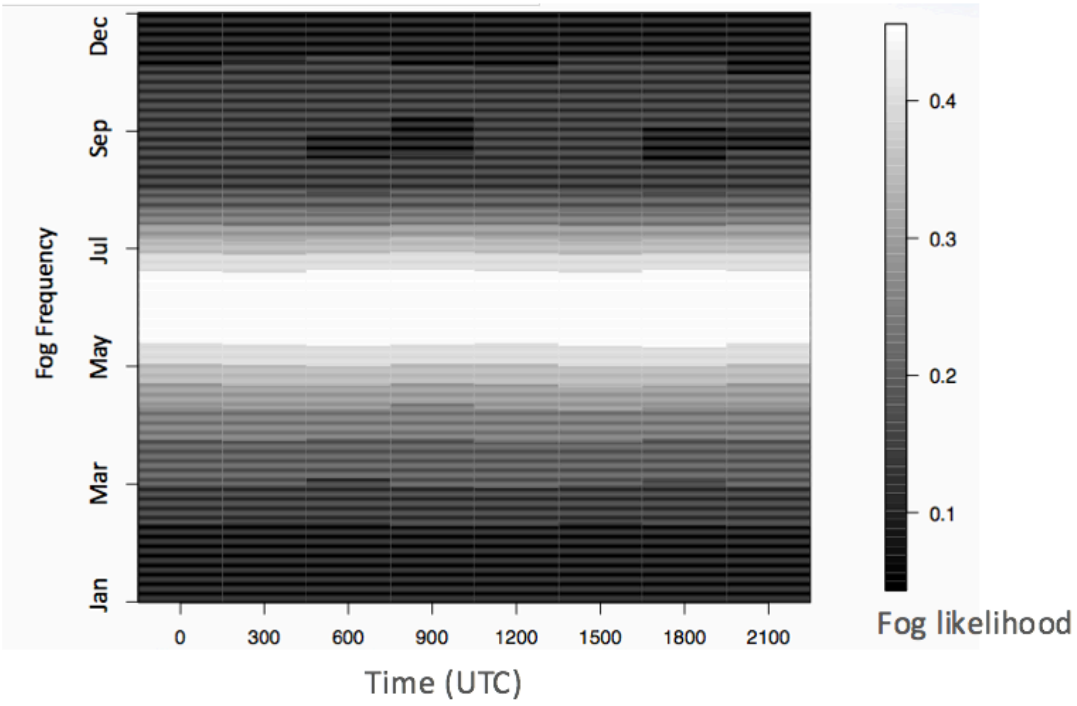

Figure 10 : A different representation of the annual and diurnal cycles captured in Figure 9. Results show strong seasonal (vertical axis) variation but only a weak diurnal cycle in fog frequency at the Grand Banks, NL.

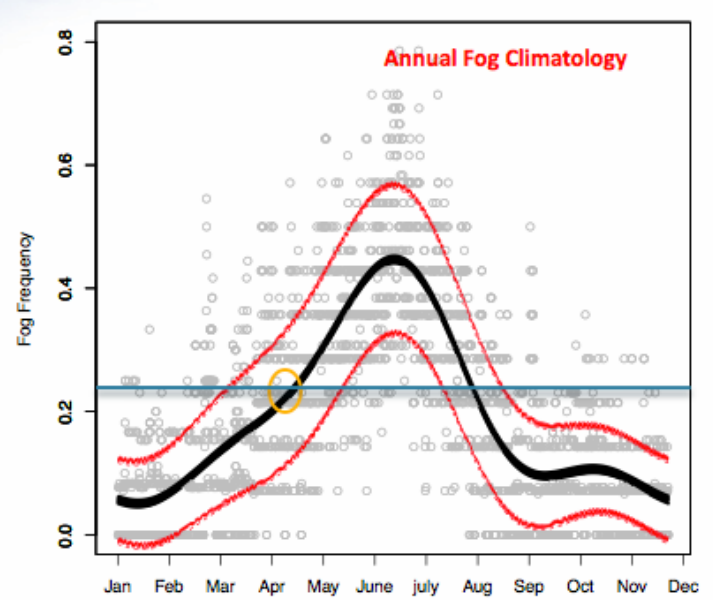

Figure 11 : Adjusts Figure 9 to highlight the climatological starting date of our defined fog season (yellow circle) and show the threshold used in this definition (frequency = 0.25).

Figure 12 gives the results of applying this definition to all available years in the Hibernia data set. Each year is shown as a vertical column, covering that year's season. Start dates show a standard deviation of 22.44 days, end dates have a standard deviation of 20.41, and the total season length has a standard deviation of 22.13 days.

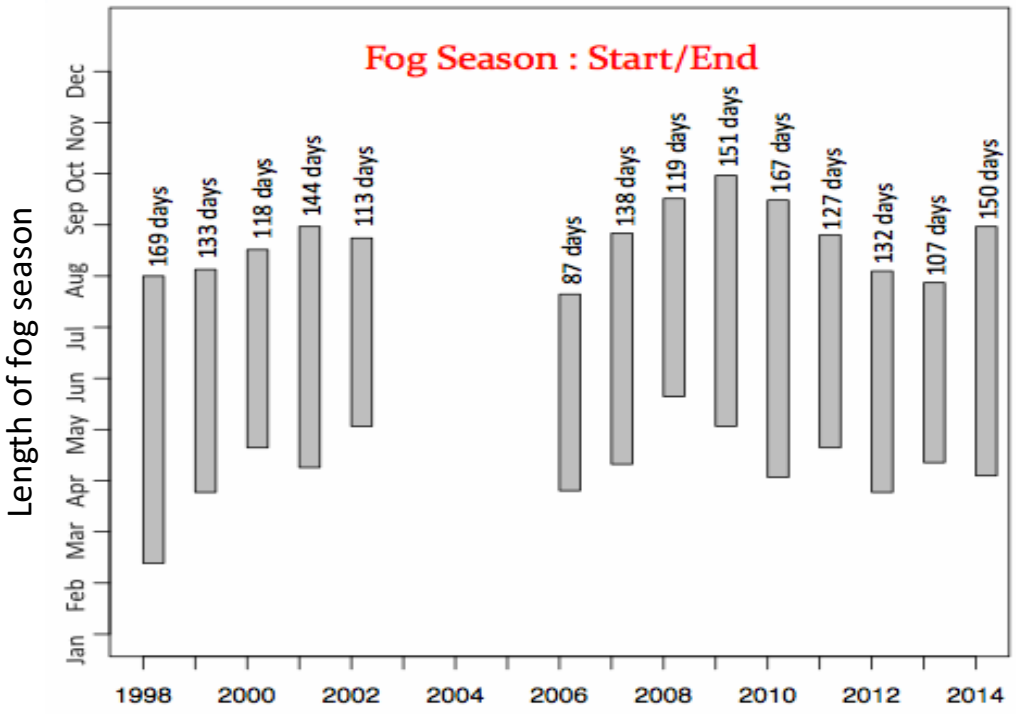

Figure 12 : Fog seasons for individual years (1998 to 2014), based on our chosen fog likelihood threshold. Gray columns mark the portion of the year associated with this season.

By calculating the number of observations that were associated with fog (ie. how common fog was during our fog seasons), the severity or intensity of a fog season can be quantified (Figure 13). This number varies from 30% of observations in the season associated with fog (2009, 2011) to as much as 43% (2010), with a mean of 34% and a standard deviation of 3.9%. Piecing this together, the Grand Banks fog season covers over one third of the year (36%), with over 34% of this season affected by significant fog (visibility < 4km). Fog conditions improve considerably into early fall, before rising again in mid-spring.

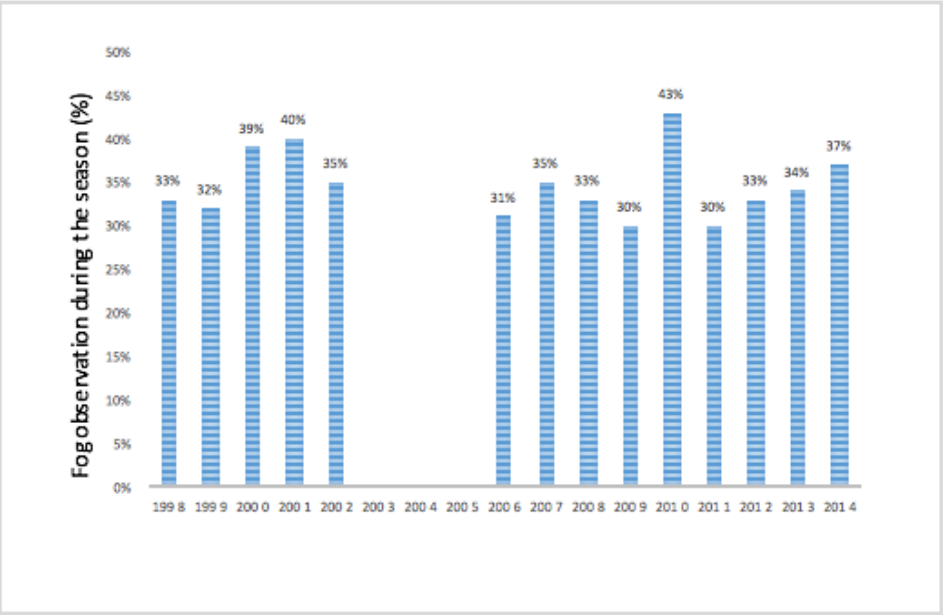

Figure 13 : Frequency of human reported fog in the MANMAR record (severity of fog season)

3.1.4 Event-Scale Climatology

Although seasonally focused fog analyses are of scientific interest and relevant for long term planning on the Grand Banks, they do not address operational concerns that typically focus on shorter time frames (a few hours to a week). Rather than asking what time of year fog is most likely to occur, many stakeholders are instead interested in whether fog will arrive or recede shortly. To begin answering these questions, it is helpful to first explore the climatology of individual fog events. For this purpose, the season was viewed as a sum of individual events that build towards our seasonal climatology. Event-level analysis allows the investigation of event duration, persistence, and frequency within the study region.

Identification of individual events was based on a declustering of visibility data, grouping fog instances into longer continuous events. Grouping began with a simple definition of 'low visibility', using the first criteria provided in section 6.1.1: visibility below 4km. Then rules were applied for grouping instances together; parameters considered included the minimum required time steps to separate events ('lull'), and an alternative minimum threshold that must be crossed before an event is considered over (which may be different than the threshold needed to initiate an event). These parameters can be adjusted to recognize that fog can change rapidly, dissipating and returning repeatedly during a single event ('patchy' fog). There is no ideal choice for these parameters, which must be set after testing and while considering possible user needs. For the purposes of this study, the event initiation and termination threshold was set to 4km visibility. The time steps requirement to consider two events separate was chosen as 9 hours (three time steps). This decision was made to avoid any unnecessary cuts in longer events due to temporary increases in visibility (fog 'lifting').

Results of the fog climatology are sensitive to criteria used to define 'fog' in MANMAR data, as well as those used to define and separate fog 'events'. For example, lowering/raising the visibility criteria influences the number of identified fog events greatly. Respectively, if the "lull" decrease to two time steps the number of events could increase or vice versa. Climatology results showed similar patterns in inter- and intra-annual variability however, suggesting that core findings are robust.

Using these parameters, 1757 low visibility 'events' were identified in the 14 years of data analyzed. Of these, 1163 could be considered 'fog' events; that is, at least part of the event met all requirements for 'fog' laid out in section 3.1.1. All low visibility events were categorized accordingly:

Minimal fog: less than 33% of the event was associated with fog.

Mixed fog: between 33% and 66% of the event was associated with fog.

Dominant fog: more than 66% of the event coincided with fog.

No Fog: a low visibility event with no reports of fog (may be caused by rain, drizzle, snow, mixed precipitation).

Figure 14 illustrates the number of each of these categories; of the 1757, 1163 were related to fog, with 530 categorized as 'fog dominant'. Minimal fog made up the second largest category (420), emphasizing that transient fog as part of more complex events is common.

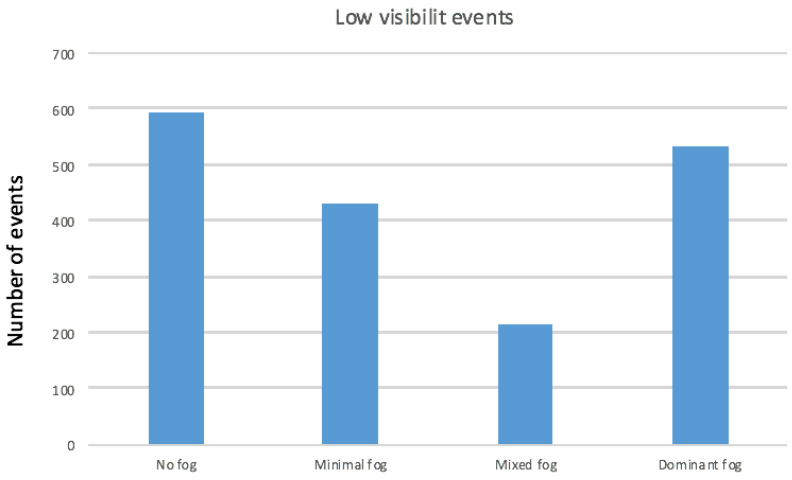

Figure 14 : Event-Scale climatology; categorizing low visibility events.

Having categorized visibility events, their key characteristics can be compared. Figures 15 and 16 compare event duration and severity as a set of boxplots, highlighting differences in mean values and outliers. Differences in duration (Fig. 15) are particularly notable; while visibility events have an average duration of two time steps (6 hrs), extreme events may last for up to two weeks (360 hours, or 120 time steps). The longest events are consistently associated with the 'Fog Dominant' category, have a mean duration of average of 24 hours and a third quartile of eighty-one hours. By comparison, minimal fog has a mean duration of one hundred and fourteen hours and third quartile of forty-two hours. As illustrated in the boxplots, these represent significant differences, with the median (black band inside the boxes) for minimum fog outside the first to third quartile in the fog dominant category.

Figure 16 shows another boxplot related to severity of the fog events, showing the fraction of each event with visibility less than one kilometer. This therefore captures the portion of the events with very severe fog. Unlike duration, our categories do not show much difference in terms of severity, with all showing a severe fog fraction of 0.5 to 0.6.

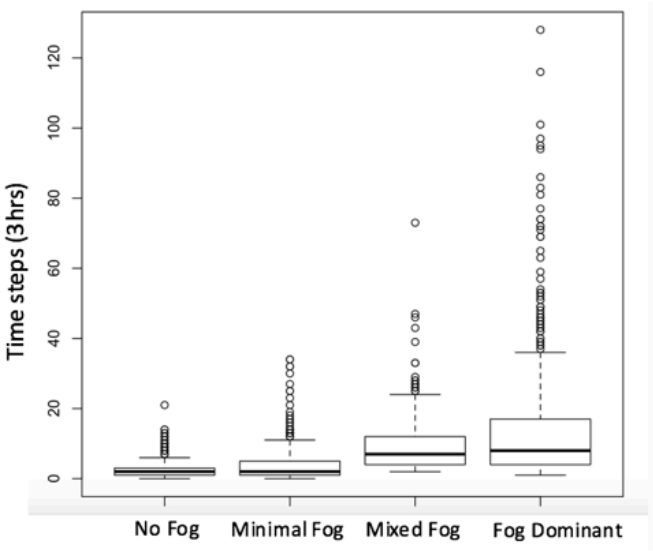

Figure 15 : Boxplots comparing event duration of different low visibility event categories.

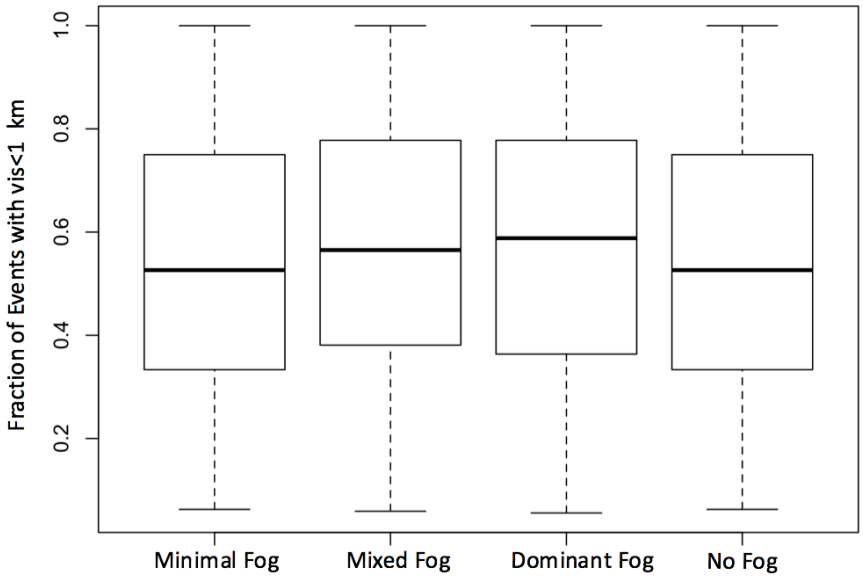

Figure 16 : Boxplots comparing event severity (fraction with visibility < 1km) of different low visibility event categories.

While categories do not appear to be distinct with respect to severity, they seem to be with respect to duration. Wilcoxon rank sum tests has been performed (Ng and Balakrishnan, 2004) to quantify the statistical significance of these duration differences. The rank sum test was chosen because it compares groups without preconceptions about statistical distributions. Sixteen between-category tests have been run, and results are given in Table 1. Results show a very clear difference in duration between Dominant Fog and most other categories, with the exception of No Fog; still, there is an 88% chance that these categories are distinct. Minimal Fog and No Fog durations are also effectively the same, but there is significant separation between Minimal and Mixed Fog. These results suggest that our categorization of visibility events on the basis of fog fraction is justified, providing sufficiently distinct differences in expected duration.

Table 1: P-values for Rank/sum result from different fog categories.

	No Fog	Minimal Fog	Mixed Fog	Dominant Fog
No Fog	1	0.48	**0.003**	0.011
Minimal Fog	0.48	1	0.014	**0.0006**
Mixed Fog	**0.003**	0.014	1	**5.007e-07**
Dominant Fog	0.01	**0.0006**	**5.007e-07**	1

3.2 Point Process

Poisson distributions are often used to model the number of independent events expected to occur in a particular time window or given interval. For example, from time t_1 to t_2, the

event count can be modelled following a Poisson distribution as $\lambda \times (t_2 - t_1)$, where λ is the event frequency (events/time) and sole parameter in the Poisson distribution. Similarly, the count over a subsequent interval t_2 to t_3, can be expected to be $\lambda \times (t_3 - t_2)$. It then follows that from t_1 to t_3 the expected count is $\lambda \times (t_3 - t_1) = \lambda \times (t_2 - t_1) + \lambda \times (t_3 - t_2)$.

In the current context, the number of expected fog events per year can be modeled using a Poisson distribution; the duration of these events might similarly be modeled using the geometric distribution. This is similar to the point process approach to modelling extreme events (Coles et al., 2001), and can be useful in determining how unusual a given fog event or season actually is. We have applied this here, beginning with annual event count data summarized in Table 2 & 3, followed by treatment of event duration.

The results show the mean event occurrence rate each year is ~83 fog events; this includes our minimal fog, mixed fog, and fog dominant event categories. The observed minimum is 68 (2008), while the maximum is 101 (1999). Fitting a Poisson distribution to these counts gives a λ of 83.07 with a standard error of 2.44; the 100-year event frequency is estimated at 105 events (+/- 5, based on two standard error deviance from the maximum likelihood estimates).

Mean event duration (again, using minimum fog through fog dominant categories) is 12.3 time steps, or over 36 hours. Respectively, the average number of time steps expected

with fog (total) in each year is 1021 time steps; this accounts for 35% of the total year. A geometric distribution was fit to durations of all fog category events; the maximum likelihood estimate of the sole distribution parameter (probability) was p = 0.075). Combining this with the expected 83 events per gives the 100-year event duration as 115 time steps (>14 days). This is apparently contradicted by the frequent occurrence of observed events with duration greater than 115 time steps in the Hibernia record (Table 3; twice in 14 years). The inference is that a geometric distribution is a poor fit to all fog events, and splitting events on the basis of physical processes or time of year may be necessary to properly assess extreme durations. This is left to later research.

Table 2: Number of fog event in each year

Year	1998	1999	2000	2001	2002	2006	2007	2008	2009	2010	2011	2012	2013	2014
Number of events	79	101	88	91	91	71	70	68	86	84	70	91	85	88

Table 3 :Event with Maximum duration(time steps) in each year

Year	*1998*	*1999*	*2000*	*2001*	*2002*	*2006*	*2007*	*2008*	*2009*	*2010*	*2011*	*2012*	*2013*	*2014*
Event with maximum duration in each year	*63*	*39*	*94*	*101*	*116*	*81*	*97*	*74*	*39*	*74*	*49*	*95*	*47*	*128*

Table 4 : Total fog events duration (time steps) in each year

Year	1998	1999	2000	2001	2002	2006	2007	2008	2009	2010	2011	2012	2013	2014
Fag duration in each year	991	935	1156	1158	1030	914	2271	970	929	1267	899	966	1019	1094

Table 5 : Poisson distribution and λ value results

Poisson distribution rate parameter	Number of events	Event with maximum duration in each year	Fog duration in each year
λ	83.07	78.35	1116.35

3.3 Summary:

The results given in this chapter clearly outline the scope of fog as a hazard at and around the Hibernia platform. Fog is frequent, particularly from spring through summer when it is expected in 25-40% of observations. It often persists for stretches of several days, and may last for two full weeks. While visibility can vary during these events, over half of an event is expected to feature visibility below 1km. Seasonal analyses and event-scale climatology's highlight the variability of both individual fog events and fog seasons viewed as whole.

Our climatological analyses suggest that fog at the Hibernia platform is primarily advection fog, as indicated by the lack of a prominent diurnal cycle that would be

expected many other forms of fog (e.g. radiation). This would also explain the strong seasonality identified in fog likelihood, as seasonal variation in key synoptic scale fields could explain much of this cycle. We expect that fog at this location has a strong connection to surface winds and sea surface temperatures; when i) sea surface temperature boundaries are strong and situated near Hibernia and ii) winds blow across this front, fog can be expected to occur. This suggests fog events are strongly connected to synoptic forcing as opposed to small scale local forces. Therefore, it is reasonable to move from viewing Hibernia fog as a local phenomenon to looking at it as an aspect of broader synoptic scale meteorology. This is the focus of next chapter.

Chapter 4

Chapter three explored the fog climatology of a single Grand Banks location in detail, focusing on information available from instruments on board the stationary Hibernia oil platform. The current chapter expands our scope to the synoptic scale (~1000 km), to identify broader environmental conditions that show a strong influence on Grand Banks fog. The following analyses are intended to highlight factors specific to this geographic location, inform efforts to improve fog prediction, and explore the potential for applying lessons learned in chapter three to other areas in the Grand Banks and global ocean.

In this chapter meteorological/oceanographic (metocean) patterns that could increase fog likelihood in the region are explored. We approach this in two separate ways. First, by estimating fog probability with data from the Hibernia climate station (logistic regression), then identifying spatial patterns that explain this probability using Canonical Correlation Analysis (CCA). This approach has been used to efficiently compare the relative usefulness of different synoptic patterns, and identify the best candidate variables for improving regional predictability. The second approach was to identify key metocean patterns, then explore the fog frequency associated with each. This was done through a synoptic classification using the method of self-organizing maps (SOM). Results deliver greater insight into large-scale factors influencing Hibernia fog and serve as secondary confirmation of the potential for synoptic scale analyses to increase fog predictability.

4.1 Identifying Relevant Synoptic Forcing:

4.1.1 Logistic Regression

In statistical analyses, regression is a process used to quantify relationships between variables. One form of regression suitable for binary variables is logistic regression (Cox, 1958), which returns the probability that the variable will take one of its two possible states. The approach is also sometimes referred to as logit regression or a logit model. While the target output of logit models is based on binary data, the input variables can be discrete, continuous or both; although not used here, the method can also be extended to predict categorical data (more than two discrete states). As with other forms of linear regression, logistic regression takes one or more independent variables as inputs and returns one or more dependent variables. In meteorology, dependent variables in this analysis are known as the predictand or response, and the independent variables are known as predictors. Applying logistic regression often starts by categorizing continuous data to give a binary predictand; a linear combination of the predictors (***x***) is then found that optimally predicts the probability the predictand will be a 'success' (category 1), such that:

$$y = f(x) = \begin{cases} 1, & \beta_0 + \boldsymbol{\beta} \cdot \boldsymbol{x} + \varepsilon > 0 \\ 0, & \text{else} \end{cases}$$

where β_o and $\boldsymbol{\beta}$ are model parameters and ε is random noise following a logistic regression. Parameters are optimized through an iterative process, aiming to maximize the

likelihood y is assigned the correct state. The cumulative probability of a success (y = 1; F($\boldsymbol{x}$)) is then given by the following logistic function

$$\mathrm{F}(x) = \frac{1}{1 + e^{-(\beta_0 + \boldsymbol{\beta} \cdot \boldsymbol{x})}}$$

There are limitations to this approach, most notably due to linearity. While the cumulative probability is nonlinear (a logistic function), it is assumed that probability will increase unidirectional as predictors increase. This is less likely to be a suitable assumption when looking at atmospheric phenomena, but may still return useful results. It can also be a useful way to reinterpret categorical data as a continuous variable (bounded between 0 and 1).

In order to apply CCA to fog probability, logistic regression has been used to estimate the probability of fog at Hibernia as a function of air temperature, dew point depression (air temperature minus dew point), and wind speed as measured at the platform. These were selected following tests of all possible combinations of variables in Table 6, evaluated with 5-fold cross-validation to prevent overfitting. The final model shows good agreement with observations, as measured with Brier scores and Relative Operating Characteristic (ROC) curves. Brier scores (Wilks & Hamill, 2007) vary from 0 (perfect) to 1 (worst case); performance here was 0.106, a 33% improvement relative to climatology. ROC performance was summarized as the area under an ROC curve (Marzban, 2004), which indicate poor performance with values below 0.5 and perfect performance with a score of 1; the current model returns 0.895. These results confirm that

logistic regression is a reasonable means of summarizing fog likelihood for the Hibernia platform.

4.1.2 CCA & Synoptic Forcing

Canonical correlation analysis (CCA) and self-organizing maps (SOMs) have been used to study synoptic scale weather patterns that promote fog on the Grand Banks. In order to do this, a 1000km (North/South) by 1000km (East/West) study domain centered over the Hibernia platform's location was examined. CCA was used to identify variables with a strong synoptic-scale association with an estimated fog likelihood (based on logistic regression, as described above). The goal here was to both i) identify spatial patterns that promote fog formation, and ii) quantify their relative value to fog prediction. A number of field variables were selected for analysis, based on their likely influence on advection fog. These include near surface air temperature (Ta), skin temperature of the ocean surface (SKT), and sea level pressure (SLP). The first two candidate variables are related to heat distribution, while the third is related to near surface winds (moving counterclockwise around low pressures and clockwise around high pressure). As a group, all are therefore strongly related to surface heat advection. These were used singly and in combination as one side of the CCA equation (**X**), while fog likelihood was used as the single variable on the other side (y). Results of CCA then provide a single pattern (in either one or more fields) that explain the greatest variation in fog likelihood, along with a correlation between the strength of that pattern and fog likelihood. In all cases, variables were first converted to spatial anomalies, removing the mean value for a given field and

date; this emphasizes the relative differences in the fields and removes influences from annual cycles.

Results are summarized as CCA correlations in Table 6, and confirm that the fields examined show a reasonable connection to fog. Notably, the synoptic-scale Ta field is the single best predictor of fog (r = 0.702), followed by SLP (r = 0.65). It is interesting that combining Ta and SKT weakens results relative to Ta alone, but combining SKT with SLP gives the best overall result (r = 0.708). Over the full year, the value of this combination is only slightly better than Ta alone (or Ta with SLP); however, during the fog season it marks a more significant improvement. The SLP & SKT combination could expect to be effective because both the heat distribution and wind field are included, capturing the primary features needed to calculate temperature advection (and therefore advection fog). In the Grand banks, fog could occur when the temperature is getting warmer than the sea surface temperature (Bullock et al. 2016). The resulting CCA pattern supports this, showing strong warm advection across an ocean temperature gradient near the Grand Banks, driven by counterclockwise wind flow around a low pressure system to the south of Newfoundland (Figure 18). The skin temperature field captured in this pattern resembles the long-term climatological mean, with a sharp boundary delineated between a cold Labrador Current to the north and a warm Gulf Stream to the south. The climatology of this pattern has shown in Figure 17. The pattern increases in strength from April through mid-July, then quickly weakens into August. The pattern is inverted (strength is negative) through fall and winter. This cycle closely follows our annual fog

climatology (Chapter 3, Figure 9), suggesting influences on Hibernia fog climatology are captured by the pattern.

Table 6 : Correlation of CCA-identified patterns with Hibernia station fog likelihood (Pr), for a range of weather variables (Ta = Air Temperature, SKT= Skin Temperature, SLP= Sea level pressure, U = zonal winds, V = meridional winds).

CCA	Correlation over the full year	Correlation within fog season
Cor (Ta, Pr)	0.702	0.500
Cor (SKT, Pr)	0.453	0.405
Cor (SLP, Pr)	0.650	0.464
Cor (SKT + Ta, Pr)	0.585	0.433
Cor (SKT + SLP , Pr)	0.708	0.588
Cor (Ta + SLP, Pr)	0.701	0.389
Cor (Ta + SLP + SKT)	0.440	0.401
Cor (Td, Pr)	0.650	0.409
Cor (UV wind , Pr)	0.464	0.386

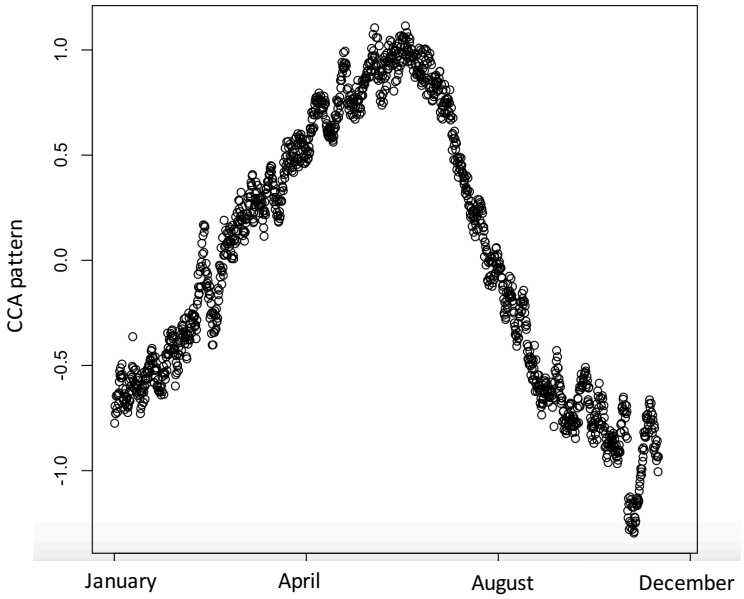

Figure 17 : Climatology (Annual Cycle) of CCA pattern's strength. Average value per day/time of year.

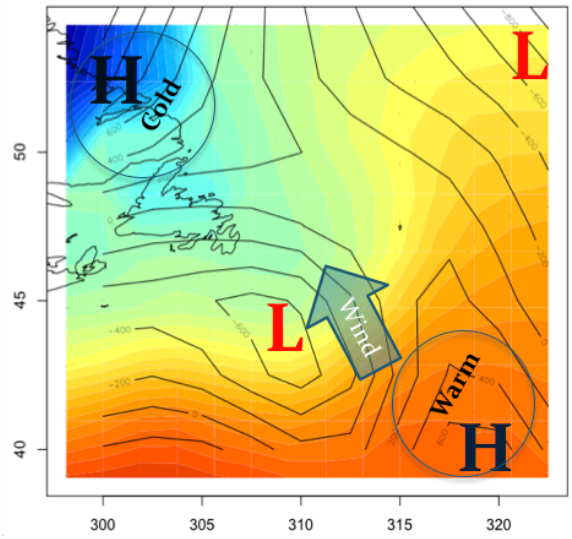

Figure 18 : CCA results show strong advection across a SST gradient, with low pressure system to the south of Newfoundland (Black lines= sea level pressure contour , Color = skin temperature). An arrow was added showing geostrophic surfaces winds expected near Hibernia.

4.1.3 Self-Organizing map

CCA provides insight into a single pattern maximally connected to fog occurrence, but little information on either the specific weather events that contribute to the pattern or what precedes/follows these events. To better explore connections between fog and SLP/SKT, self-organizing maps (SOM) were used to codify daily synoptic sea level pressure and skin temperature data for the Grand Banks. This approach constructs a joint synoptic climatology of the two fields, summarizing available daily data as a small set of key archetypal patterns (e.g. Hewitson and Crane 2002). The number of these key patterns (SOM nodes) must be considered carefully, as a compromise between detail (more patterns) and interpretability (fewer patterns); a small number may give results that are too general, while more patterns will capture more detail but may become difficult to interpret. SOM users also must test a wide range of training parameters, including training rate, neighborhood size, and the number of training steps.

For the current study, a 6 by 8 SOM has been selected after testing with a range of sizes, each trained multiple times with different training parameters. Results were compared quantitatively using quantization error (Cottrell & Fort, 1986), which is simply a measure of the mean difference between observations used in training and the best matching SOM node. A lower quantization error implies a specific SOM is a better fit to the original data. It cannot be used to compare SOMs of different sizes, as the value inevitably drops as SOM size increases. It is, however, useful in comparing SOMs with comparable node

numbers. SOMs of all sizes were also qualitatively compared using Sammon mapping (Sammon 1969). A Sammon map gives a two dimensional representation of multidimensional points that preserves the relative Euclidean distance between the points. It is useful in choosing a SOM because it gives a sense of whether or not a SOM is well ordered. Poorly ordered (and difficult to interpret) SOMs will give a Sammon map that appears to twist or fold, putting nodes that are far apart on the SOM lattice close to one another on the Sammon map. A well-ordered, easy to interpret SOM will appear 'flat'.

Results of the selected SOM are shown in Figure 19; a Sammon map for this SOM is shown in Figure 20. Each node in the SOM shows SLP patterns as black contour lines and SKT patterns as colour contours. The organization in the SOM is apparent as a tendency for neighbouring nodes to resemble one another. This allows us to refer to neighbouring nodes on the basis of the features they share. A brief summary of the broad patterns found in the nodes follows.

The upper right of the SOM most closely resembles CCA results (rows 0 and 1, columns 5 through 7; or [0:1, 5:7]), with a low pressure system south/southeast of Newfoundland and a strong skin temperature gradient. Most of these would promote southerly winds and warm advection near the Grand Banks. Very different patterns in the lower left of the SOM ([4:5, 6:7]) would likely promote similar winds and advection, with a paired high pressure system to the west of our domain and low pressure system in the northwest (Labrador Sea). Winds on the left side of the SOM would blow in the opposite direction, promoting northerly winds and cold advection near the Grand Banks. These are

dominated by higher pressures in the southwest (lower left) or northwest (upper left), usually with low pressure near Greenland. Skin temperature and SLP gradients in these nodes are both weaker, potentially limiting their potential to produce cold advection fog events. The middle columns of the SOM show transitions between these left-side and right-side patterns, with the lower middle ([3:5, 2:5]) moving southwesterly highs toward the western end of the domain and the upper middle ([0:2, 2:5]) show the west/northwest track of southwesterly lows or the displacement of Greenland lows with highs.

In contrast with SLP, skin temperatures in the SOM nodes vary little in spatial distribution. Nodes are instead distinguished mostly by the strength of temperature gradients in what appears as a fairly consistent spatial pattern. There may be some small, regionally important differences in the position of the front between warm water to the south/southeast and cold water to the north/northwest, but these are difficult to identify in this large, multivariate SOM.

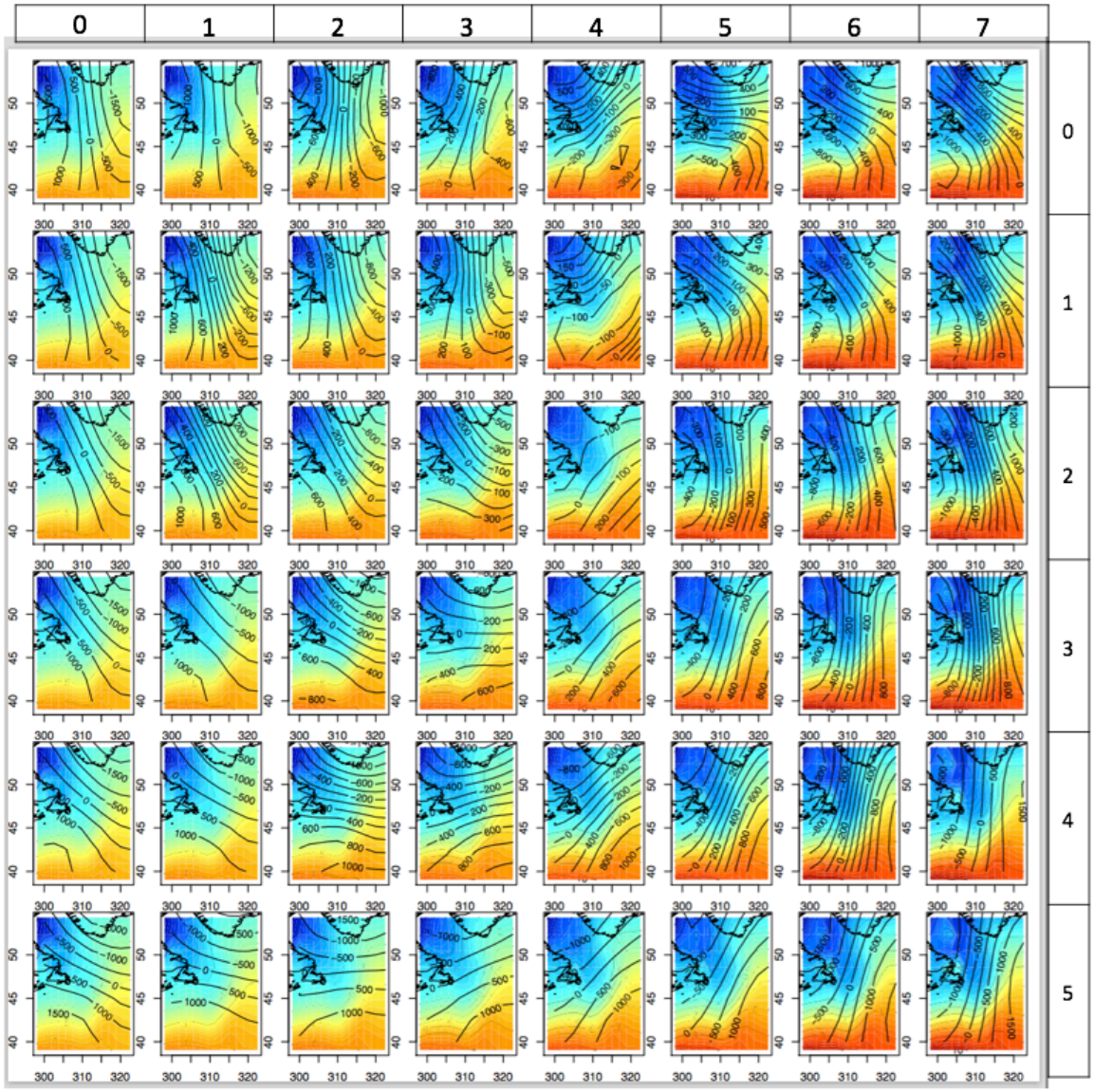

*Figure 19 : A 6*8 SOM of Sea Level Pressure and Skin Temperature for the Grand Banks (1998-2014). Each image represents a single SOM node. Contour lines represent SLP and contour colors represent SKT.*

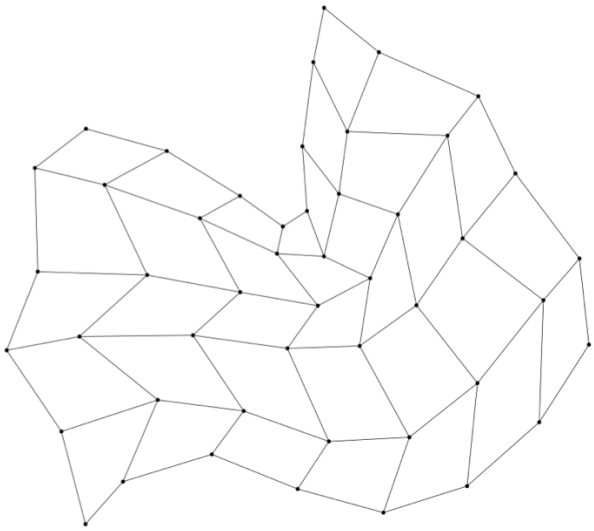

Figure 20 : Sammon map for the final trained SOM with lowest the Quantization error.

4.2 Synoptic Climatology:

Each daily average of the SLP and SKT anomaly fields from the reanalysis data can be associated with a single node on the SOM. The occurrence frequency of each node can then be calculated as the number of times each node occurs divided by the total number of daily input data; alternately, nodes can be compared on the number of occurrences rather than a fractional occurrence. This has been done, with results shown in Figure 21 (occurrences over the full year) and Figure 22 (occurrences over just the climatological fog season, or April 8 to August 21). From information like this we can determine which nodes (and associated weather patterns) dominate over a full year and which occur more often during our fog season. By further matching observed fog events to specific nodes, the relative frequency of fog and the frequency of fog occurrence for each node are calculated (figure 23).

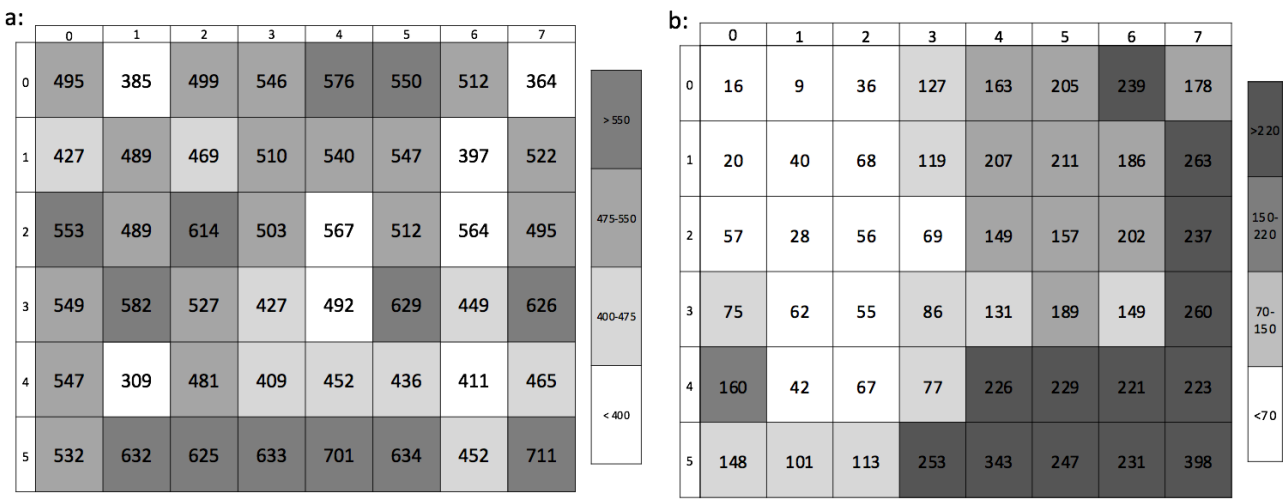

Figure 21 : Figure 21a shows the study region's synoptic climatology, summarized as the count of each node occurrence over the full study period. Figure 21b focuses on synoptic climatology of fog events only, showing the number of times fog was reported while a given node occurred.

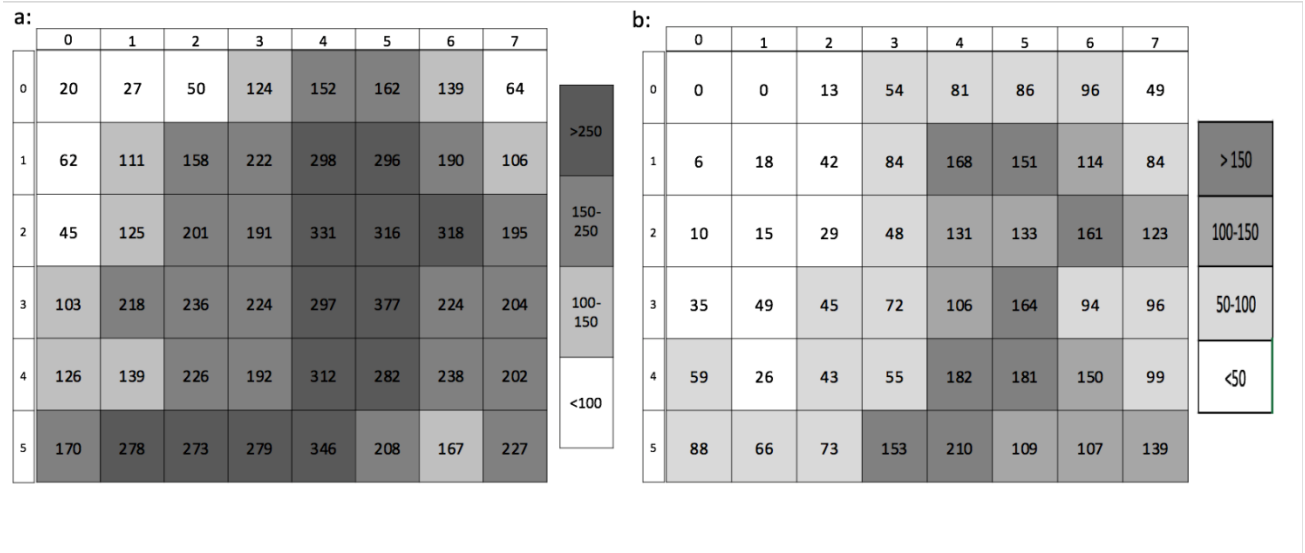

Figure 22 : Same as Figure 21, but looking only the climatological Hibernia fog season (April, 8 to August,21), rather than the full year.

The results show that over the course of a full year all SOM nodes have a high likelihood of occurring (Fig. 21a), with total node occurrence counts between 301 [4,1] and 711 [5,7]. The fog season, however, favors nodes in the middle and bottom of the SOM (Fig. 5a). Nodes in the upper left occur rarely during this period, suggesting northerly winds are much less common than strong southerly winds.

Results also show strong physical consistency in nodes associated with fog events. Fog event counts in Figures 21 and 22 are highest in nodes near one another (right, lower right), which share similar features. Nodes showing high fog counts confirm the combination of a strong north/south temperature gradient with a southerly wind direction are the strongest factors driving summer advection fog formation. It is also notable from Figure 22 that summer fog can coincide with high winds near Hibernia, as the nodes favored during fog typically show a very strong pressure gradient. However, it is also clear that fog can occur for any node over the full year (Figure 21b); and nearly any node during the peak fog season (Figure 22b; the exceptions are [0, 0:1]). This suggests that northerly winds drive cold advection fog ([1,1], [2,1]), although these are rarer than warm advection events. Weak sea level pressure patterns and/or westerly winds (bottom left side of the map) are also connected with lower fog frequencies. As a whole, these results support the findings of CCA analysis, pointing to a combination of strong southerly winds with a strong temperature gradient as the key factor in occurrence of fog, while also highlighting the fact that fog can (and does) occur with other synoptic set-ups.

4.3 Summary

Overall, SOM and CCA analyses point to the strength and position of synoptic pressure systems (and the resulting winds) as the critical synoptic-scale element influencing Hibernia fog. Skin temperature also exerts an influence, but displays less variability in the current analyses that could explain fog occurrence. From these results we can infer that it is critical for the prediction of fog to track the specific paths of pressure systems in the vicinity of the Grand Banks. SOM analysis suggests that systems tracking from the Gulf of St. Lawrence towards Greenland or the open North Atlantic are particularly likely to produce fog, which may last for days with slower moving systems. Strong pressure gradient force (closely packed isobars) in fog-affected SOM nodes further confirm that high surface winds do not significantly deter Hibernia fog, at least during periods when skin temperature gradients are strong. Instead, gentle winds (particularly from the north or west) appear to reduce fog likelihood, indicating that cold advection fog is much less common than warm advection, or more easily dissipated by wind mixing. Ongoing data collection at and around the Hibernia platform will facilitate further investigation into synoptic forcing of Grand Banks fog, and may help improve global marine fog forecasting in the future.

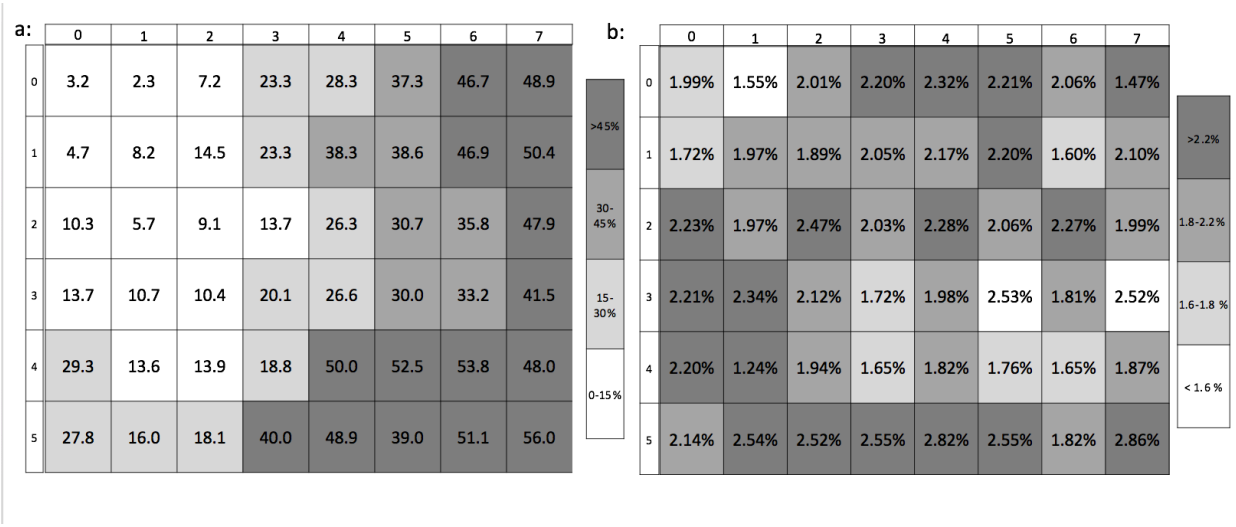

Figure 23 : Right table shows probability of fog occurrence at each node (%), left table shows the relative frequencies of occurrence at each nodes.

Open questions remain with respect to the influence of factors other than winds & SLP. CCA tests with skin and surface air temperature confirm that these factors influence fog, if not as strongly as SLP. This should be explored with dedicated CCA and SOM analyses over a smaller domain, where slight (but regionally important) fluctuations in temperatures are less likely to be hidden by bigger variations between the Labrador Sea and Gulf Stream.

With respect to generalizing results to areas outside of the Grand Banks, our results suggest that sufficiently strong temperature advection is enough to produce thick Grand Banks-type fog. There may be other locally important factors that allow this to happen,

such as boundary layer heights, vertical stability, or a favorable range of temperatures across the ocean gradient that promote these events. With further research, it is possible that a new fog-typing and automated forecasting system could be developed for ocean areas near a strong temperature contrast.

Chapter 5

5.1 Summary and Discussion

Frequent and severe fog events pose significant economic, health and operational concerns to marine industry activities on the Grand Banks of Newfoundland. Since the oil/gas industry and commercial fisheries are expanding in this region, the Grand Banks has significant economic importance. Our aim in this research was to provide a necessary climatological baseline for improving fog forecasting and predictability, in order to reduce economic and health impacts in the area.

In order to provide a solid foundation for our research, a full fog climatology for the Hibernia oil platform has been established, the location with the longest meteorological observations in the Grand Banks. Analyses included consideration of frequency, severity and duration of low visibility events. Results show that fog in the region demonstrates a weak diurnal cycle, which means fog frequency is relatively independent of the time of the day. This suggests the region is dominated by advection fog, which is less likely to show strong diurnal dependency than most other forms forms of fog (e.g. radiation). Hibernia fog does however show a significant annual cycle, with strong seasonality and notable high fog frequency from spring through the summer months. These results are not confirmed previous finding, and past studies along the Canadian east coast (Gultepe et al., 2009) and the Grand Banks (Taylor, 1917) have highlighted the frequent advection marine fog, due to converges the Gulf stream and either the Labrador current or cool coastal waters. However, our research shows much less diurnal influence than coastal Nova Scotia (Shearwater; Gultepe et al, 2009), possibly due to increased emphasis on

advection fog on the Grand Banks, or at least advection fog unconnected to predictable diurnal winds (sea breezes; a possible factor in coastal locations). We also provide a more detailed outline of fog's influence on the Grand Banks than has previously been available, including analyses of variability in fog season durations and severity, building Taylor's pioneering research (Tylor, 1917).

While seasonal and annual analyses have some meteorological value, we expect that many stakeholders impacted by fog are more concerned with specific events, particularly their onset and duration. For this reason, the climatology of fog events was further explored. Event-scale concerns were addressed by viewing the fog season as a set of discrete fog events, declustering visibility data to identify periods of near-continuous low visibility. This approach allows the investigation of event duration, persistence (i.e. consistency of low visibility), and frequency within the study region. These event-scale analyses acknowledge that low visibility events in our study area may be associated with weather conditions other than (or in combination with) fog (e.g. rain and/or snow). For this reason, low visibility events have been categorized according to their quantified association with fog ('no fog' through 'fog dominant' events). Although the criteria for these categories was set subjectively, they show some statistically significant differences in duration, with mean category duration varying from a few hours (minimal fog) to over a day (dominant fog); extreme durations (e.g up to 360 hrs) are disproportionately associated with 'fog dominant' low visibility conditions.

Statistical modeling of event frequency and duration was conducted by treating fog as a point process. Results give a mean annual event occurrence rate of ~83; the 100-year event frequency is estimated at 105 events. Mean event duration was found to be 36 hours which, combined with mean event frequency, gives an average number of fog hours in each year as 1020 time steps. Performing an extreme duration analysis proved difficult, and will likely require additional analysis beyond the scope of the current project.

Further analyses used to investigate the broader synoptic scale fog events connects occurrence with synoptic conditions. A combination of Canonical Correlation Analysis (CCA) and Self-Organizing Maps (SOM) was used to identify weather patterns that influence fog formation on the Grand Banks. Skin temperature and sea level pressure (SLP) combined with fog probability appears to explain fog probability better than other fields examined; which makes sense for advection fog, since skin temperature and SLP reflect the two key aspects of heat advection (temperature gradients and winds respectively). A CCA-identified skin temperature/SLP pattern that best explains fog likelihood further shows conditions that would promote strong temperature advection across the Grand Banks. The climatological strength of this pattern closely matches our annual cycle of fog likelihood, suggesting it is a true reflection of synoptic patterns influencing fog.

It should be noted that the CCA-derived correlations leave much of fog likelihood unexplained ($r = 0.59$ in fog season, or 25% explained variation). This is partly explained by uncertainty in the logistic regression used to quantify fog likelihood, but it is important

to point out that fog is a microphysical process. With respect to synoptic forcing, the relatively low correlation likely reflects this. Other dynamical considerations are likely less important than cloud microphysics and complex boundary layer processes, acting on scales much smaller than synoptic. Keeping this in mind, the CCA correlations are likely much higher than would be expected in regions where non-advection fog is common.

Also, from SOM results we can point to the strength and position of synoptic pressure systems as a critical element affecting Grand Banks fog formation. This implies that it is necessary to track paths of these pressure systems through the region to accurately predict fog events. SOM results also suggest that systems tracking from the Gulf of St. Lawrence towards Greenland or the open North Atlantic are particularly likely to produce fog. These trajectories may last for days with slower moving systems, explaining the long duration of many fog events. Results further indicate that high surface winds don't have a negative impact on fog formation, as long as skin temperature gradients are sufficiently strong in the region.

The synoptic analyses presented here are preliminary work, and could be built on with additional work. CCA tests suggest additional variables and alternated spatial domains may offer greater predictability than the simple large-domain SLP and skin temperature fields used here. In particular, a smaller domain skin temperature may reveal the influence of slight fluctuations in temperatures currently hidden by bigger variations between the Labrador Current and Gulf Stream. It is also important to note that any future CCA analysis would benefit from more accurate estimates of fog likelihood (use here as

one of the paired CCA variates). These could benefit from additional station-scale observations, from both Hibernia and other offshore platforms in the region. Local factors such as boundary layer heights, vertical stability, and the range of temperature across the ocean gradient might improve the accuracy of our fog likelihood estimates, improving our ensuing spatial analyses; adding additional platforms could also help generalize results across the broader Grand Banks (rather than limiting us to Hibernia).

Future analysis is likely to benefit from both longer records of observation (as Hibernia is still operating), more observation sites (with the newly operational Hebron platform and others), and more consistent data collection and archiving. New observing tools including ceilometers and updated visibility sensors are being deployed, and platform operators are increasing their commitments to meteorological/oceanographic observation and archiving. As a result, future fog research may have fewer problems interpreting human-reported weather conditions and identifying false reports.

At the moment, research continues on season-specific synoptic fog analyses, and developing a better system for classifying low visibility events on the basis of fog 'types'. This is currently being pursued in collaboration with AMEC Foster Wheeler, a consulting group that provides meteorological forecasts for the offshore oil industry. Results of the current work have also informed on-going development of statistical post-processing approaches to improving Numerical Weather Prediction fog forecasts. The logit models used to estimate fog likelihood represent the simplest version of these post-processing techniques, and more advanced versions based on various machine learning techniques

are currently being tested. Although the research presented in this thesis represent only the first steps towards an improved understanding of (and capacity to predict) Grand Banks fog, it has also proven critical to these ongoing efforts.

6 Bibliography

Allan, S. S., Gaddy, S. G., & Evans, J. E. (2001). Delay causality and reduction at the New York City airports using terminal weather information systems (No. ATC-291). Cambridge, Mass, USA: Lincoln Laboratory, Massachusetts Institute of Technology.

Alhoneimi, E., Hollmen, J., Simula, O., and Vesanto, J. (1998). Process monitoring and modelling using the self-organising map. Helsinki University of Technology, Laboratory of computer and information science, Finland.

Alhoneimi, E., Simula, O., and Vesanto, J. (1997). Analysis of complec systems using the Self-organising map. Helsinki University of Technology, Laboratory of computer and information science, Finland.

Astel, A., Tsakovski, S., Barbieri, P., & Simeonov, V. (2007). Comparison of self-organizing maps classification approach with cluster and principal components analysis for large environmental data sets. Water Research, 41(19), 4566-4578.

Avotniece, Z., Klavins, M., & Lizuma, L. (2015). Fog climatology in Latvia. Theoretical and applied climatology, 122(1-2), 97-109.

Back, B, Sere, K and Hanna, V (1998) Managing complexity in large database using self-organising map. Accounting management and information technologies, 8:191-210

Barry, RG and, Perry, A, H (2001) Synoptic climatology and its applications. In: Barry RG and Carleton AM (eds) Synoptic and Dynamic Climatology. London: Routledge: 547–603.

Belorid, M., Lee, C., Kim, J., & Cheon, T. (2015). Distribution and long-term trends in various fog types over South Korea. Theoretical & Applied Climatology, 122(3/4), 699-710. doi:10.1007/s00704-014-1321-x

Bendix, J (2002). A satellite-based climatology of fog and low-level stratus in Germany and adjacent areas. Atmos Res 64:3–18.

Bretherton, C. S., Smith, C., & Wallace, J. M. (1992). An intercomparison of methods for finding coupled patterns in climate data. Journal of climate, 5(6), 541-560.

Blogs Nosey Parker. (n.d.). Retrieved July 26, 2017, from http://blogs.canoe.com/parker/2010/11/05.

Brown, J. R., Jakob, C., & Haynes, J. (2010). Rainfall frequency and intensity over Australia and their association with the atmospheric circulation in a global climate model. Journal of Climate, 23(24), 6504-6525.

Bullock, T., Isaac, G. A., Beale, J., & Hauser, T. (2016, October 24). Improvement of Visibility and Severe Sea State Forecasting on the Grand Banks of Newfoundland and Labrador. Offshore Technology Conference. doi:10.4043/27406-MS

Cavazos, T. (2000). Using self-organizing maps to investigate extreme climate events: An application to wintertime precipitation in the Balkans. Journal of climate, 13(10), 1718-1732.

Cereceda, P., Osses, P., Larrain, H., Farıas, M., Lagos, M., Pinto, R., & Schemenauer, R. S. (2002). Advective, orographic and radiation fog in the Tarapacá region, Chile. Atmospheric Research, 64(1), 261-271.

Choi, H., Seo, J. W., & Kim, C. S. (2000). Numerical prediction on sea surface drift induced by windstorm in the coastal complex terrain. Korean J. Atmos. Sci, 3, 67-82.

Croft, P. J. (2003). Fog. Encyclopedia of atmospheric sciences. Academic, San Diego, 777-792.

Coles, S., Bawa, J., Trenner, L., & Dorazio, P. (2001). An introduction to statistical modeling of extreme values (Vol. 208). London: Springer.

Cottrell, M., & Fort, J. C. (1986). A stochastic model of retinotopy: A self-organizing process. Biological Cybernetics, 53(6), 405-411.

Cox, DR (1958). "The regression analysis of binary sequences (with discussion)". J Roy Stat Soc B. 20: 215–242. JSTOR 298389

Finnis, J., Cassano, J., Holland, M., Serreze, M., & Uotila, P. (2009). Synoptically forced hydroclimatology of major Arctic watersheds in general circulation models; Part 1: the Mackenzie River Basin. International Journal of Climatology, 29(9), 1226-1243.

Furrer, E. M., Katz, R. W., Walter, M. D., & Furrer, R. (2010). Statistical modeling of hot spells and heat waves. Climate Research, 43(3), 191-205.

García, H. L., & González, I. M. (2004). Self-organizing map and clustering for wastewater treatment monitoring. Engineering Applications of Artificial Intelligence, 17(3), 215-225.

Gultepe, I., Tardif, R., Michaelides, S. C., Cermak, J., Bott, A., Bendix, J., & ... Cober, S. G. (2007). Fog Research: A Review of Past Achievements and Future Perspectives. Pure & Applied Geophysics, 164(6/7), 1121-1159. doi:10.1007/s00024-007-0211-x

Gultepe, I., Pagowski, M., & Reid, J. (2007). A satellite-based fog detection scheme using screen air temperature. *Weather and forecasting*, *22*(3), 444-456.

Gultepe, I., Hansen, B., Cober, S. G., Pearson, G., Milbrandt, J. A., Platnick, S., ... & Oakley, J. P. (2009). The fog remote sensing and modeling field project. *Bulletin of the American Meteorological Society*, *90*(3), 341-359.

Hansen, B., Gultepe, I., King, P., Toth, G., & Mooney, C. (2007, January). Visualization of seasonal-diurnal climatology of visibility in fog and precipitation at Canadian airports. In AMS Annual Meeting, 16th Conf. Appl. Climatology, San Antonio, Texas (pp. 14-18).

Hewitson, B. C., & Crane, R. G. (2002). Self-organizing maps: applications to synoptic climatology. Climate Research, 22(1), 13-26.

Higgins, M. E., & Cassano, J. J. (2010). Response of Arctic 1000 hPa circulation to changes in horizontal resolution and sea ice forcing in the Community Atmospheric Model. Journal of Geophysical Research: Atmospheres, 115(D17).

Hilliker, J. L., & Fritsch, J. M. (1999). An observations-based statistical system for warm-

season hourly probabilistic forecasts of low ceiling at the San Francisco International Airport. Journal of Applied Meteorology, 38(12), 1692-1705.

Hyvärinen, O., Julkunen, J., & Nietosvaara, V. (2007). Climatological tools for low visibility forecasting. In Fog and Boundary Layer Clouds: Fog Visibility and Forecasting (pp. 1383-1396). Birkhäuser Basel.

Kalnay, E., Kanamitsu, M., Kistler, R., Collins, W., Deaven, D., Gandin, L., ... & Zhu, Y. (1996). The NCEP/NCAR 40-year reanalysis project. Bulletin of the American Meteorological Society, 77(3), 437-471.

Kalteh, A. M., Hjorth, P., & Berndtsson, R. (2008). Review of the self-organizing map (SOM) approach in water resources: Analysis, modelling and application. Environmental Modelling & Software, 23(7), 835-845.

Kangas, J., and Simula, O. (1995). Precess monitoring and visualization using self-organising map. Chapter 14 in (ed. Bulsari, A B) Neural Networks for chemical Engineers, Elsevier Science publishers.

Katz, R. W., Parlange, M. B., & Naveau, P. (2002). Statistics of extremes in hydrology. Advances in water resources, 25(8), 1287-1304.

Kim, C. K., & Yum, S. S. (2010). Local meteorological and synoptic characteristics of fogs formed over Incheon international airport in the west coast of Korea. Advances in Atmospheric Sciences, 27(4), 761-776.

Kohonen, T., Oja, E., Simula, O., Visa, A., & Kangas, J. (1996). Engineering applications of the self-organizing map. Proceedings of the IEEE, 84(10), 1358-1384.

Kohonen, T. (1982). Self-organized formation of topologically correct feature maps. Biological cybernetics, 43(1), 59-69.

Kohonen, T. (2001). Self-organizing maps Springer. Berlin, Germany.

Koračin, D., & Dorman, C. E. (2001). Marine atmospheric boundary layer divergence and clouds along California in June 1996. *Monthly Weather Review*, *129*(8), 2040-2056.

Koračin, D., Lewis, J., Thompson, W. T., Dorman, C. E., & Businger, J. A. (2001). Transition of stratus into fog along the California coast: Observations and modeling. Journal of the atmospheric sciences, 58(13), 1714-1731.

Koračin, D., Businger, J.A., Dorman, C.E., Lewis, J.M. (2005). Formation, evolution, and dissipation of coastal sea fog. Bound. -Layer Meteorol. 117, 447–478.

Koračin, D., Dorman, C. E., Lewis, J. M., Hudson, J. G., Wilcox, E. M., & Torregrosa, A. (2014). Marine fog: A review. Atmospheric Research, 143, 142-175.

Kyle P. R., Aster R., Crain J., Dunbar N., Esser R., McIntosh W. C., Richmond M., Ruiz M., and Wardell L. J. (2003). Monitoring Volcanic Activity at Mount Erebus, Antarctica. IX International Symposium on Antarctic Earth Science.

Lebart, L., Morineau, A., & Warwick, K. M. (1984). Multivariate descriptive statistical analysis; correspondence analysis and related techniques for large matrices. New York: John Wiley.

Leipper, D.F. (1994). Fog on the U.S. West Coast, a review. Bull. Am. Meteorol. Soc. 72, 229–240.

Lewis, J.M., Koračin, D., Rabin, R., Businger, J. (2003). Sea fog off the California coast: viewed in the context of transient weather systems. J. Geophys. Res. Atmos. 108 (D15), 4457. http://dx.doi.org/10.1029/2002JD002833.

MANOBS. (2006), Manual of surface weather observations, meteorological service of Canada, environment canada. Available online at http://www.mscsmc.ec.gc.ca/msb/manuals_e.cfm. 369 pp.

Marzban, C. (2004). The ROC curve and the area under it as performance measures. Weather and Forecasting, 19(6), 1106-1114.

Meyer, M.B., Jiusto, J.E., Lala, G.G. (1980). Measurements of visual range and radiation-fog (haze) microphysics. J. Atmos. Sci. 37, 622–629.

Ng, H. K. T., & Balakrishnan, N. (2004). Wilcoxon-type rank-sum precedence tests. Australian & New Zealand Journal of Statistics, 46(4), 631-648.

Tadross, M. A., Hewitson, B. C., & Usman, M. T. (2005). The interannual variability of the onset of the maize growing season over South Africa and Zimbabwe. Journal of climate, 18(16), 3356-3372.

Tippett, M. K., & Barnston, A. G. (2008). Skill of multimodel ENSO probability forecasts. Monthly Weather Review, 136(10), 3933-3946.

Obu-Cann, K., Fujimura, K., Tokutaka, H., Ohkita, M., Inui, M., & Ikeda, Y. (2001). Data mining of power transformer database using self-organising maps. In Info-tech and Info-net, 2001. Proceedings. ICII 2001-Beijing. 2001 International Conferences on (Vol.

4, pp. 44-49). IEEE.

Phillips, D. W. (1990). The Climates of Canada (available from Environment Canada, Downsview, Ontario), Minister of Supply and Services Canada, 40-42

Penn, B. S. (2005). Using self-organizing maps to visualize high-dimensional data. Computers & Geosciences, 31(5), 531-544.

Pook M. J., McIntosh, P. C., & Meyers, G. A. (2006). The synoptic decomposition of cool-season rainfall in the southeastern Australian cropping region. Journal of Applied Meteorology and Climatology, 45, 1156– 1170

Rauthe, M., Kunz, M., & Kottmeier, C. (2010). Changes in wind gust extremes over Central Europe derived from a small ensemble of high resolution regional climate models. Meteorologische Zeitschrift, 19(3), 299-312.

Rencher, A. C. (1992). Interpretation of canonical discriminant functions, canonical variates, and principal components. The American Statistician, 46(3), 217-225.

Repelli, C. A., & Nobre, P. (2004). Statistical prediction of sea-surface temperature over the tropical Atlantic. International Journal of Climatology, 24(1), 45-55.

Reusch, D. B., Alley, R. B., & Hewitson, B. C. (2005). Relative performance of self-organizing maps and principal component analysis in pattern extraction from synthetic climatological data. Polar Geography, 29(3), 188-212.

Rustum, R. (2009). Modelling Activated Sludge Wastewater Treatment Plants Using Artificial Intelligence Techniques, PHD thesis, School of Built Environment, Heriot-Watt University, April 2009.

Sammon, J. W. (1969). A nonlinear mapping for data structure analysis. IEEE Transactions on computers, 100(5), 401-409.

Saunders, P. M. (1964). Sea smoke and steam fog. Quarterly Journal of the Royal Meteorological Society, 90(384), 156-165.

Sheridan, S. C., & Lee, C. C. (2011). The self-organizing map in synoptic climatological research. Progress in Physical Geography, 35(1), 109-119.

Sirabella, P., Giuliani, A., Colosimo, A., & Dippner, J. W. (2001). Breaking down the climate effects on cod recruitment by principal component analysis and canonical correlation. Marine Ecology Progress Series, 216, 213-222.

Souders, C. G., & Renard, R. J. (1984, June). The visibility climatology of McMurdo/Williams Field, Antarctica. In 10th conference on Weather Forecasting and Analysis, Clearwater Beach, FL. American Meteorological Society.

Suckling, P. W., & Mitchell, M. D. (1988). Fog climatology of the Sacramento urban area. The Professional Geographer, 40(2), 186-194.

Sugimoto, S., Sato, T., & Nakamura, K. (2013). Effects of synoptic-scale control on long-term declining trends of summer fog frequency over the pacific side of Hokkaido island. Journal of Applied Meteorology and Climatology, 52(10), 2226-2242. doi:10.1175/JAMC-D-12-0192.1

Tanimoto, Y., Xie, S. P., Kai, K., Okajima, H., Tokinaga, H., Murayama, T., ... & Nakamura, H. (2009). Observations of marine atmospheric boundary layer transitions across the summer Kuroshio Extension. Journal of Climate, 22(6), 1360-1374.

Tardif, R., & Rasmussen, R. M. (2007). Event-based climatology and typology of fog in the New York City region. Journal of applied meteorology and climatology, 46(8), 1141-1168.

Taylor, G.I., (1915). Eddy motion in the atmosphere. Philos. Trans. R. Soc. Lond. Ser. A 215, 1–26.

Taylor, G. I. (1917). The formation of fog and mist. *Quarterly Journal of the Royal Meteorological Society*, *43*(183), 241-268.

Tippett, M.K., Barnston, A.G. (2008). Skill of multi-model ENSO probability forecasts. Monthly Weather Review (136), 3933–3946.

Tremant, M. (1987). La prévision du brouillard en mer. Météorologie Maritime et Activities Océanographique Connexes. Rapport No. 20. TD no. 211. World Meteorological Organization, Geneva, Switzerland.

Tymvios, F. S., Michaelides, S. C., & Skouteli, C. S. (2008). Estimation of surface solar radiation with artificial neural networks. In Modeling solar radiation at the earth's surface (pp. 221-256). Springer Berlin Heidelberg.

Uyeda, H., & Yagi, T. (1982). Observation of sea fogs at Kushiro in eastern Hokkaido. Bosai Kagaku Gijutsu Kenkyujo Kenkyu Hokoku (Report of the National Research Institute for Earth Science and Disaster Prevention), 69-92.

Valdez, J (2000). National Weather Service—A high impact agency . . . we make a

difference: Reinvention goals for 2000. National Weather Service. Retrieved from http://govinfo.library.unt.edu/npr/library/announc/npr5.htm.

Van den Dool, H. M. (1994). Long-range weather forecasts through numerical and empirical methods. Dynamics of atmospheres and oceans, 20(3), 247-270.

Van Schalkwyk, L., 2011: Fog forecasting at Cape Town International Airport: A climatological approach. M.S. dissertation, Dept. of Geography, Geoinformatics and Meteorology, University of Pretoria, 133 pp.

Van Schalkwyk, L., & Dyson, L. L. (2013). Climatological characteristics of fog at cape town international airport. Weather and Forecasting, 28(3), 631-646.

Veljović, K., Vujović, D., Lazić, L., & Vučković, V. (2015). An analysis of fog events at Belgrade International Airport. Theoretical & Applied Climatology, 119(1/2), 13-24. doi:10.1007/s00704-014-1090-6

Vesanto, J., Himberg, J., Alhoniemi, E., & Parhankangas, J. (2000). SOM toolbox for Matlab 5. Helsinki University of Technology, Finland.

Wallace, J. M., & Hobbs, P. V. (2006). Atmospheric science: an introductory survey (Vol. 92). Academic press, New York.

Ward, M. N. (1998). Diagnosis and short-lead time prediction of summer rainfall in tropical North Africa at interannual and multidecadal timescales. Journal of Climate, 11(12), 3167-3191.

Westcott, N. (2004, January). Synoptic conditions associated with dense fog in the Midwest. In *Proc. 14th Conf. on Applied Climatology*.

Whiffen, B., Delannoy, P., & Siok, S. (2004, May). Fog: Impact on road transportation and mitigation options. In National Highway Visibility Conference, Madison, Wisconsin, USA.

Willett, H. C. (1928). Fog and haze, their causes, distribution and forecasting. *Monthly Weather Review*, 56 (11), W. B. No. 971. Retrieved from https://pdfs.semanticscholar.org/0552/394c4135666bfe4fe9fa7a54c14ed00024cd.pdf

Wilks, D. S. (2001). A skill score based on economic value for probability forecasts. Meteorological Applications, 8(2), 209-219.

Wilks, D. S., & Hamill, T. M. (2007). Comparison of ensemble-MOS methods using GFS reforecasts. Monthly Weather Review, 135(6), 2379-2390.

Wu, Y, Pelot, R.P, Hilliard, C. (2009). The influence of weather conditions on the relative incident rate of fishing vessels. Risk Anal, (7), 985-99. doi: 10.1111/j.1539-6924. 2009. 01217. x.

Xoplaki, E., Luterbacher, J., Burkard, R., Patrikas, I., & Maheras, P. (2000). Connection between the large-scale 500 hPa geopotential height fields and precipitation over Greece during wintertime. Climate research, 14(2), 129-146.

Zhang, L, Scholz, M, Mustafa, A, Harrington, R (2009) application of self-organizing map as a prediction toll for an integrated constructed wetland agro ecosystem treating agriculture runoff, Bio resource Technology, 100(2): 559-565.